Calculation of Blade-to-Blade Flow in a Turbomachine by Streamline Curvature

By D. H. WILKINSON

Central Electricity Generating Board

Reports and Memoranda No. 3704*

December, 1970

Summary

The object of a blade-to-blade method is to calculate the blade surface velocity distribution and the outlet angle for a given three-dimensional cascade. These give the heat drop or work done and indicate whether shock waves are likely to occur. A boundary layer calculation can then also be done to estimate the profile loss and to see if separation is likely and how much laminar flow there might be. Most methods available at present can only deal with special cases such as two-dimensional compressible flow or three-dimensional incompressible flow. The nearest alternative approach to a complete method, using a through flow method, has a longer run time and cannot find the outlet angle.

A new method is described in this report for calculating the compressible flow in a three-dimensional cascade of blades. This uses the 'stream line curvature' technique with tangential quasi-orthogonals, and the shapes of the stagnation streamlines are determined iteratively to satisfy the condition of periodicity in the tangential direction. This condition is also sufficient to determine the outlet angle. The calculation includes all effects of compressibility, change of annulus area and change of radius, enabling deviations due to velocity ratio and Coriolis forces to be found. Comparisons of theoretical predictions with those of other theories and with experiment for particular cases show good agreement.

A new design method for calculating the blade shape required for a prescribed velocity distribution is also outlined as a simple extension to the analysis method.

These methods can be applied to cascades in steam, gas and water turbines, gas circulators, compressors and pumps with axial, mixed or radial flow.

* Replaces A.R.C. 32 878.

LIST OF CONTENTS

1. Introduction

The solution of the problem of calculating the compressible inviscid flow through a three-dimensional cascade, defined by the intersection of an arbitrary meridional stream surface of varying thickness with a blade row is usually attempted by one of two main approaches, the matrix method, or streamline curvature. There is wide agreement on the general equations of momentum, continuity, etc., governing the flow and the methods differ in the numerical techniques used for solving the equations and applying the boundary conditions. A recent paper by Smith and Frost[1] (1970) has described the 'matrix' method in which the flow equations are combined into one equation for the stream function, in the form of a Poisson's equation of which the right hand side is determined iteratively as the calculation proceeds. The unknowns are the stream function values at points on a non-uniform grid covering the flow field. The method as published does not find the outlet angle, although this is not a fundamental limitation and further development may enable it to do so. Solutions published so far have been verified only for two-dimensional cases with stream surface thickness variation although as it stands the method should be able to include change of radius effects for fixed or rotating blades. A disadvantage at present is the long run times but this is probably mainly due to using a computer that is too slow and has inadequate storage, and it is expected that run times will be reduced. A more important limitation is that the form of the equation for the stream function prevents calculations with any supersonic flow, and the convergence of the method would also be expected to be significantly worse at high Mach numbers. There is at present, no very obvious way round this Mach Number limitation, although one may of course be found.

The other main approach for solving the equations is the 'streamline curvature' technique. This appears in two forms, one using normals to the flow, Jansen[2], and Bindon and Carmichael[3], (1970) and the other using quasi-orthogonals, Katsanis[4,5] (1964), (1965), Wilkinson[6] (1970). The methods using normals have, as far as is known, only been used for two-dimensional cases, but are for a number of reasons probably less good than the quasi-orthogonal methods. A quasi-orthogonal, or q-o as it will be referred to, is a fixed line which is in practice nearly always straight, but is not necessarily so, and which goes from one wall to the other of the channel confining the flow. All of the mass flow therefore crosses it and this is used to satisfy the continuity equation by adjusting the velocity level along the q-o' to give the correct mass flow. The velocity distribution along the q-o' is given by the velocity gradient equation which is derived from the equations of momentum, entropy and energy. As all of the terms on the right hand side of the velocity gradient equation are not known, an iterative procedure is used to solve the equations simultaneously. It has been shown in Wilkinson[6] (1970) that the method can include supersonic flow in patches which occupy up to half the channel and by Bindon and Carmichael[3] (1970) that the method can be extended to isentropic supersonic flow for the 'normals' method.

In Wilkinson[6] (1970) a two-dimensional method was described in which q-o's approximately normal to the flow were used. A difficulty was encountered in deciding on the correct shape for the upstream and downstream stagnation stream lines (s.s.l.). Although the flow goes through an infinite cascade the method only considers the flow through one channel, defined within the blade row by the suction and pressure surfaces of adjacent blades and outside the blade row by the s.s.l.'s. In Katsanis[5] (1965) and Wilkinson[6] (1970) the s.s.l. shapes must be estimated, but it is shown in Wilkinson and Allsopp[7] (1969) that this can cause considerable errors, particularly for compressible flow. The reason for this can easily be seen by considering a nozzle blade Fig. 10 for which over the last half of the suction surface, where the Mach Number is highest, the channel is formed by the suction surface itself on one side and the s.s.l. from the trailing edge on the other. At high Mach Numbers small variations in channel width due to errors in the s.s.l. shape have a large effect, an area reduction of only 4 per cent being sufficient to raise the mean Mach Number from 0·8 to 1·0. Apart from difficulties with choking, the load at the trailing edge will not reduce to zero and the velocity gradients along the blade surfaces will be incorrect. There is no simple way of estimating the s.s.l. shapes as these depend on the blade shape, the Mach Number on annulus area changes, which make the s.s.l.'s curve, and on relative vorticity or Coriolis force effects for a rotating blade row. However, it is possible to determine the s.s.l. shapes by using the condition of periodicity. This condition is simply that for an infinite array of blades, all flow parameters are periodic in the tangential direction with a wavelength equal to the pitch of the blades. Two points at the same

axial or meridional stations on the 'suction' and 'pressure' stagnation streamlines are in effect the same point and should have the same velocities and other flow parameters. This condition has been given by Smith and Frost (1970), among others, where it is used as a part of a two-dimensional stream line curvature method although no information is given there on how the s.s.l. shapes are found, and the published examples do not verify its successful operation.

This report will show the derivation of the velocity gradient equation in the most suitable form for tangential q-o's. The stability and accuracy of the solution will be analysed and an expression for the optimum damping factor derived. A new method will be given for iteratively determining the shapes of the stagnation streamlines, and also of the outlet angle by means of a Kutta–Joukowski condition. The methods for finding first and second derivatives and of smoothing will also be discussed and recommendations made. Finally, a number of comparisons of the method with other theories and with experiment will be shown for special cases which indicate the accuracy of the new method when applied to general compressible flow blade-to-blade cases with change of radius and annulus area and fixed and rotating blades.

Also a new design method will be suggested in which the procedure for calculating the stagnation streamline shapes will be extended to modify the blade shape as well as to obtain a prescribed suction surface velocity distribution.

2. Equations and Method of Solution

2.1. Velocity Gradient Equation

An equation for the gradient of relative velocity W in the θ-direction to give the velocity distribution along a tangential q-o' is required. Consider a cylindrical coordinate system (z, r, θ) fixed in space and a coordinate system (z, r, θ') rotating with the blades at angular velocity ω, where ω is positive in the θ-direction, Fig. 1.

The momentum equation is

$$\frac{1}{r}\frac{d(V_\theta r)}{dt} = -\frac{1}{\rho r}\frac{\partial p}{\partial \theta}. \tag{1}$$

The entropy equation is

$$T\frac{\partial s}{\partial \theta} = \frac{\partial h}{\partial \theta} - \frac{1}{\rho}\frac{\partial p}{\partial \theta}. \tag{2}$$

Eliminating p between (1) and (2)

$$\frac{1}{r}\frac{d(V_\theta r)}{dt} = \frac{T}{r}\frac{\partial s}{\partial \theta} - \frac{1}{r}\frac{\partial h}{\partial \theta}, \tag{3}$$

h can be replaced using Euler's turbine equation for points on a streamline

$$h_{t_1} - \omega r V_{\theta 1} = h_{t_2} - \omega r V_{\theta 2} = I$$

or

$$h_t = I + \omega r V_\theta \tag{4}$$

and the energy equation

$$h_t = h + \frac{V^2}{2}. \tag{5}$$

From (4) and (5)

$$h = I + \omega r V_\theta - \frac{V^2}{2}. \tag{6}$$

Also, from the two coordinate systems

$$\theta = \theta' + \omega t \tag{7}$$

$$r\frac{\partial \theta}{\partial t} = r\frac{\partial \theta'}{\partial t} + \omega r$$

or

$$V_\theta = W_\theta + \omega r. \tag{8}$$

Defining a meridional velocity V_m by

$$V_m^2 = V_z^2 + V_r^2, \tag{9}$$

it follows that

$$V^2 = V_m^2 + V_\theta^2 \tag{10}$$

or from (8)

$$= V_m^2 + W_\theta^2 + 2\omega r W_\theta + \omega^2 r^2$$

$$= W^2 + 2\omega r W_\theta + \omega^2 r^2, \tag{11}$$

where

$$W^2 = V_m^2 + W_\theta^2. \tag{12}$$

From (6), (8) and (11)

$$h = I + \frac{\omega^2 r^2}{2} - \frac{W^2}{2}. \tag{13}$$

It will be assumed (i) that there is uniform inflow so that $\partial I/\partial\theta = 0$, (ii) that the flow is within a meridional stream surface which is a surface of revolution so that

$$\frac{\partial r}{\partial \theta} = 0,$$

and (iii) that tangential entropy gradients may be neglected, $\partial s/\partial\theta = 0$. Assumption (ii) is the usual one of neglecting stream surface twist. Assumption (iii) neglects entropy gradients due to losses within the boundary layers. It does not prevent $\partial s/\partial m$ being non-zero and in fact losses of this type will come in via the continuity equation, in the form of reduced pressure and density and hence in increased velocity level, and it is important to put them in to get the right velocities and enthalpy changes.

With these assumptions (13) gives

$$\frac{1}{r}\frac{\partial h}{\partial \theta} = -\frac{1}{2r}\frac{\partial W^2}{\partial \theta}$$

and (3) becomes

$$\frac{W}{r}\frac{\partial W}{\partial \theta} = \frac{1}{r}\frac{d(V_\theta r)}{dt} = \frac{1}{r}\frac{d(W_\theta r + \omega r^2)}{dt}, \tag{14}$$

since $V_\theta = V_\theta(z, r, \theta, t)$ and $W_\theta = W_\theta(z, r, \theta')$, it is convenient to express the total derivative in terms of partial derivatives with respect to the rotating coordinate system (z, r, θ') to avoid time dependence. Therefore

$$\frac{W}{r}\frac{\partial W}{\partial \theta} = V_r\frac{\partial W_\theta}{\partial r} + \frac{W_\theta V_r}{r} + 2\omega V_r + \frac{W_\theta}{r}\frac{\partial W_\theta}{\partial \theta'} + V_z\frac{\partial W_\theta}{\partial z}. \tag{15}$$

From the definition of distance m along the meridional stream surface implied by (9)

$$\frac{\partial}{\partial m} = \cos\alpha\frac{\partial}{\partial z} + \sin\alpha\frac{\partial}{\partial r}$$

or

$$V_m\frac{\partial}{\partial m} = V_z\frac{\partial}{\partial z} + V_r\frac{\partial}{\partial r}$$

and (15) becomes

$$\frac{W}{r}\frac{\partial W}{\partial \theta} = V_m\frac{\partial W_\theta}{\partial m} + \frac{W_\theta V_r}{r} + 2\omega V_r + \frac{W_\theta}{r}\frac{\partial W_\theta}{\partial \theta'}.$$

Similarly, defining distance along a stream line, s, by

$$ds^2 = dm^2 + r^2\,d\theta'^2,$$

$$W\frac{d}{ds} = V_m\frac{\partial}{\partial m} + \frac{W_\theta}{r}\frac{\partial}{\partial \theta'}$$

and

$$\frac{W}{r}\frac{\partial W}{\partial \theta} = W\frac{dW_\theta}{ds} + \frac{W_\theta V_r}{r} + 2\omega V_r \tag{16}$$

where dW_θ/ds is the convective derivative of W_θ along a streamline. Noting that $dm/ds = \cos\beta = V_m/W$ (16) can be written

$$\frac{W}{r}\frac{\partial W}{\partial \theta} = V_m\frac{dW_\theta}{dm} + \frac{W_\theta V_r}{r} + 2\omega V_r. \tag{17}$$

Equation (17) for the velocity gradient can be shown to be the same as that given by Katsanis[5] (1965) and may also be found from the condition of zero absolute vorticity about an element of the meridional stream surface

Equation (17) may also be written

$$\frac{\partial W}{\partial \theta} = \cos\beta\left\{\frac{d(W_\theta r)}{dm} + 2\omega r\frac{dr}{dm}\right\}. \tag{18}$$

If used in this form, determination of the right hand side involves 'double differentiation' in the sense of Wilkinson[6] (1970). Since the distribution of W is found as a result of an iteration, W_θ can only be found from this by

$$W_\theta = W\sin\beta,$$

with β from

$$\tan\beta = r\frac{d\theta}{dm}.$$

This involves numerical calculation of $d\theta/dm$ followed by a second numerical differentiation of W_θ. This 'double differentiation' process was shown in Wilkinson[6] (1970) to be rather inaccurate and to involve a particular and hidden smoothing process which may be neither necessary nor desirable. More flexibility is obtained by making the second derivative $d^2\theta/dm^2$ appear directly in the equation.

Since

$$W_\theta = V_m\tan\beta = V_m r\frac{d\theta}{dm}$$

$$W_\theta r = V_m r^2\frac{d\theta}{dm},$$

and (18) becomes

$$\frac{\partial W}{\partial \theta} = \cos\beta\left\{\frac{d(V_m r^2)}{dm}\frac{d\theta}{dm} + V_m r^2\frac{d^2\theta}{dm^2} + 2\omega r\frac{dr}{dm}\right\}. \tag{19}$$

Equation (19) is the form of the velocity gradient equation used. Numerical differentiation is considered in Section 2.5. The procedure with equation (19) is to start with the value of $W_{i,NM}$ on the midstream line from the previous iteration and to integrate numerically in both directions using the trapezium rule to find the velocity distribution from suction to pressure surface. After this it is necessary to adjust the velocity level to satisfy continuity and this is done by adding a constant ΔW at all of the streamlines. It is not necessary to recalculate $\partial W/\partial\theta$ until the iteration is complete and a new set of stream lines has been found.

2.2. Continuity and Losses

Considering the meridional stream surface to have a thickness $\Delta r = \Delta r(m)$, Fig. 1, the mass flow crossing any q-o' considering one flow channel only, is

$$M_N = \int_{\theta_1}^{\theta_N} \rho W\cos\beta\cos\alpha\Delta r\,.\,r\,.\,d\theta, \tag{20}$$

where subscripts 1 and N indicate the suction and pressure surfaces, or their associated stagnation streamlines, respectively. In front of or behind the blade row

$$\theta_N - \theta_1 = \frac{2\pi}{NB}$$

where NB is the number of blades. Within the blade row

$$\theta_N - \theta_1 = \frac{2\pi}{NB} - \theta_t \tag{21}$$

where θ_t is the local tangential thickness of the blade in radians.

Total enthalpies along a streamline are found by (4) or, in relative quantities

$$h_{t_r} = I + \frac{\omega^2 r^2}{2} = h_{t_r}(m) \tag{22}$$

then

$$h = h_{t_r} - \frac{W^2}{2}. \tag{23}$$

It is useful to work in terms of relative quantities as losses may be estimated approximately from fixed two-dimensional cascade tests as a loss coefficient which is the relative total pressure loss divided by the outlet relative dynamic pressure. At any point, assuming a perfect gas,

$$p_{t_r} = p_{t_{\text{ref}}}\left(\frac{h_{t_r}}{h_{t_{\text{ref}}}}\right)^{\gamma/(\gamma-1)} - \Delta p_{t_r} \tag{24}$$

where subscript ref indicates reference values, say at inlet, and Δp_{t_r} is the loss in relative total pressure which must be estimated from loss correlations or boundary layer calculations.

The total pressure loss through the whole blade row is usually input as a loss coefficient non-dimensionalised with respect to relative dynamic pressure at outlet. This loss must be distributed in some way through the channel and the simple assumption is made that it varies linearly in terms of distance along the mid-stream line from zero at the leading edge, $i = ML$ to a maximum at the trailing edge $i = MT$ and is constant at zero and the maximum in front of and behind the blade row respectively.

The relative total density then follows from the gas law

$$\rho_{t_r} = \frac{\gamma}{(\gamma-1)J}\frac{p_{t_r}}{h_{t_r}} \tag{25}$$

and the static density from the isentropic relation

$$\rho = \rho_{t_r}\left(\frac{h}{h_{t_r}}\right)^{1/(\gamma-1)} = \rho_{t_r}\left(1 - \frac{W^2}{2h_{t_r}}\right)^{1/(\gamma-1)}. \tag{26}$$

Equations (22), (24), (25) and (26) enable the static density to be found and substituted in equation (20) to find the mass flow.

Equation (20) is more conveniently written

$$\overline{M}_N = \frac{M_N}{\cos\alpha \,.\, \Delta r \,.\, r \,.\, (\theta_N - \theta_1)} = \frac{1}{(\theta_N - \theta_1)}\int_{\theta_1}^{\theta_N} \rho W \cos\beta \, d\theta, \tag{27}$$

since all of the quantities in the denominator of $\overline{M}_N$ are known as functions of z and $\overline{M}_N$ can be found at the start of the calculation for each q-o'.

In general a given W distribution in (27) will not give the correct $\overline{M}_N$ and an increment ΔW at all points along the q-o' must be added. To find ΔW we need

$$\frac{d\overline{M}_N}{dW}$$

which is approximately

$$\frac{d\overline{M}_N}{dW} \simeq \cos\beta_{NM}\frac{d(\rho W)_{NM}}{dW}.$$

From (26)

$$\left.\begin{aligned}\frac{d\overline{M}_N}{dW} &\simeq \left\{\cos\beta \,.\, \rho_{t_r}\left[1-\left(\frac{\gamma+1}{\gamma-1}\right)\frac{W^2}{2h_{t_r}}\right]\left[1-\frac{W^2}{2h_{t_r}}\right]^{(2-\gamma)/(\gamma-1)}\right\}_{NM}\\ \text{or, alternatively, in terms of } \rho\\ \frac{d\overline{M}_N}{dW} &\simeq \left\{\cos\beta \,.\, \rho\left[1-\left(\frac{\gamma+1}{\gamma-1}\right)\frac{W^2}{2h_{t_r}}\right]\Big/\left[1-\frac{W^2}{2h_{t_r}}\right]\right\}_{NM},\end{aligned}\right\} \tag{28}$$

where subscript NM indicates the mid-stream line.

Equations (27) and (28) are used to find ΔW and the iteration process repeated until ΔW is negligible.

For q-o's on which Mach Numbers near or above 1·0 may be reached it is advisable to evaluate

$$\frac{d(\rho W)}{dW}$$

at all points on the q-o, and use

$$\frac{dM_N}{dW} = \frac{1}{(\theta_N-\theta_1)}\int_{\theta_1}^{\theta_N}\cos\beta\frac{d(\rho W)}{dW}d\theta.$$

This is because if the q-o' intersects a supersonic patch at a high angle, the velocity could be subsonic at both ends and supersonic in the middle without it being choked. For highly inclined q-o's then the Mach Number on the mid-streamline may not be a good enough guide to whether it is choked or not, and the exact expression for dM_N/dW given above should be used.

For choking $dM_N/dW = 0$ and from (28)

$$W^{*2} = \left(\frac{\gamma-1}{\gamma+1}\right).2h_{t_r}. \tag{29}$$

The speed of sound is given by

$$a^2 = (\gamma-1)h = h_{t_r}.(\gamma-1)\left[1-\frac{W^2}{2h_{t_r}}\right].$$

Therefore

$$a^{*2} = h_{t_r}(\gamma - 1)\left[1 - \frac{\gamma - 1}{\gamma + 1}\right]$$

$$= \left(\frac{\gamma - 1}{\gamma + 1}\right) . 2h_{t_r}$$

and therefore

$$M_{\text{rel}}^{*2} = \frac{W^{*2}}{a^{*2}} = 1{\cdot}0.$$

This shows that choking occurs approximately at a relative Mach Number of 1·0 on the mid-streamline, and that supersonic flow on less than half the q-o' can exist without choking the q-o' as a whole. This enables the method to deal with supersonic patches. There are of course two possible distributions of W that satisfy equation (27), except actually at choking. These are the subsonic and supersonic values. Either can be found using equations (26), (27), and (28), the one that appears depending on whether the initial W_{NM} taken is less than or greater than W^* from equation (29). This assumes that the supersonic flow is isentropic, which will only be true in the absence of shock waves. Supersonic q-o's will only exist following a sonic throat and the extent of the supersonic region will depend on the downstream pressure.

2.3. Stability and Convergence

In order to ensure convergence and minimise the number of iterations required it is necessary to determine the optimum damping factor. In Wilkinson[6] (1970), Katsanis[5] (1965), and Katsanis[4] (1964) the change in streamline position between one iteration and the next was multiplied by a factor less than 1·0 to prevent divergence of the calculation process. Wilkinson[6] (1970), explained the reason for this and gave an expression for the optimum damping factor in the two-dimensional case with q-o's roughly normal to the flow. This stability analysis was extended to axisymmetric cases in Wilkinson[8] (1969). However in applying this to multi-stage turbomachines it was found necessary to damp the change in velocity gradient instead of the change in streamline position and the same procedure will be followed here.

The simple flow model for the stability analysis is shown in Fig. 2 where the exact solution is a uniform helical flow about a constant radius cylinder. The coordinate system in the meridional stream surface is usually (m, θ') but another useful non-dimensional one is (ξ, θ') where

$$\xi = \int \frac{1}{r} dm. \tag{30}$$

This gives a conformal transformation of the flow in the meridional stream surface, which generally has double curvature, onto a flat plane in which all flow and geometrical angles are preserved.

The exact values of $\partial W/\partial\theta'$ in Fig. 2 are zero and a perturbation will be assumed of the form

$$\Delta\frac{\partial W}{\partial\theta'} = K . \frac{4}{q_N^2}(q . q_N - q^2) \cos\frac{2\pi}{\lambda}(m - m_0)$$

where $q = \theta' - \theta'_1$, and K is a constant.

Since it was found in Wilkinson[6] (1970) that the phase of the error component had no effect on the result, we will take $m = m_0$ at q-o' zero.

Then at q-o' zero,

$$\Delta\frac{\partial W}{\partial\theta'} = K . \frac{4}{q_N^2}(q . q_N - q^2).$$

Integrating,

$$W = W_1 + \int_0^q \Delta \frac{\partial W}{\partial \theta'} = W_1 + \frac{4K}{q_N^2}\left(q_N \frac{q^2}{2} - \frac{q^3}{3}\right). \tag{31}$$

Neglecting the small variation in β from q_1 to q_N a stream function ψ is defined by

$$\psi = \int_0^q \rho W \cos \beta r \, dq$$

or

$$\bar{\psi} = \frac{\psi}{r \cos \beta \bar{\rho}} = \int_0^q \frac{\rho W}{\bar{\rho}} dq,$$

putting

$$\frac{\rho W}{\bar{\rho}} \simeq \overline{W} + (W - \overline{W})\bar{c} = (1 - \bar{c})\overline{W} + \bar{c}W$$

where,

$$\bar{c} = \frac{1}{\bar{\rho}} \overline{\frac{d(\rho W)}{dW}}. \tag{32}$$

Then

$$\bar{\psi} = (1 - \bar{c})\overline{W}q + \bar{c} \int_0^q W \, dq. \tag{33}$$

From (31) and (33),

$$\bar{\psi} = (1 - \bar{c})\overline{W}q + \bar{c}W_1 q + \frac{4\bar{c}K}{q_N^2}\left(q_N \frac{q^3}{6} - \frac{q^4}{12}\right).$$

To satisfy continuity, put $\bar{\psi} = \overline{W}q_N$ at $q = q_N$, from which

$$W_1 = \overline{W} - \frac{Kq_N}{3}.$$

Therefore

$$\left.\begin{aligned} \bar{\psi} &= \left(\overline{W} - \frac{Kq_N\bar{c}}{3}\right)q + \frac{4\bar{c}K}{q_N^2}\left(q_N \frac{q^3}{6} - \frac{q^4}{12}\right) \\ \text{and} \quad \frac{\partial \bar{\psi}}{\partial q} &= \overline{W} - \frac{K\bar{c}q_N}{3} + \frac{4\bar{c}K}{q_N^2}\left(q_N \frac{q^2}{2} - \frac{q^3}{3}\right). \end{aligned}\right\} \tag{34}$$

The position of the mid-streamline, $\psi = \overline{W}q_N/2$ is found by approximating to the ψ distribution near $q = q_N/2$ by

$$\psi \simeq \psi_{q_N/2} + \left(q - \frac{q_N}{2}\right)\left(\frac{\partial\psi}{\partial q}\right)_{q_N/2}$$

from which

$$q \simeq \frac{q_N}{2} + \frac{\psi - \psi_{q_N/2}}{\left(\frac{\partial\psi}{\partial q}\right)_{q_N/2}} \tag{35}$$

From (34) and (35) the mid-streamline is at

$$q = \frac{q_N}{2} + \frac{5}{48}\frac{K\bar{c}q_N^2}{\overline{W}},$$

so the displacement from the correct position is $\frac{5}{48}(K\bar{c}q_N^2/\overline{W})$. There are similar displacements at neighbouring q-o's with the same wavelength and waveform as the velocity gradient error, and the new velocity gradient can be calculated from the streamline shape by equation (19) which, for this case, reduces to

$$\frac{\partial W}{\partial\theta} = \cos\beta\left\{r^2\frac{d\theta}{dm}\frac{dV_m}{dm} + V_m r^2\frac{d^2\theta}{dm^2}\right\} \tag{36}$$

or, neglecting the first term, considered below.

$$\frac{\partial W}{\partial\theta} = \cos^2\beta\,\overline{W}r^2\frac{d^2\theta}{dm^2}$$

the calculated streamline positions are used to find $d^2\theta/dm^2$ and hence the new $\partial W/\partial\theta$ from this equation. For the calculated streamline displacements

$$\frac{d^2\theta}{dm^2} = \frac{5}{48}\frac{k}{h^2}\frac{K\bar{c}q_N^2}{\overline{W}}$$

where $k = k(\lambda/h)$ depends on the numerical differentiation method used, *see* Wilkinson[6] (1970), and new

$$\frac{\partial W}{\partial\theta} = K\,.\,\frac{5}{48}k\bar{c}\left(\frac{rq_N}{h}\right)^2\cos^2\beta.$$

This is the new $\partial W/\partial\theta$ on the mid-streamline and compares with the original value of K.
Change in $\partial W/\partial\theta$ due to the iteration is therefore

$$-K(1 - \tfrac{5}{48}k\bar{c}\cos^2\beta A^2),$$

and since the correct change is $-K$ the initial error can be reduced to zero by factoring the calculated change by

$$f = \frac{1}{1 - \frac{5}{48}k\bar{c}\cos^2\beta A^2} \tag{37}$$

where

$$A = \frac{r(\theta_N - \theta_1)}{h}.$$

From equations (28) and (32) it can be shown that

$$\bar{c} = 1 - M_{\text{rel}}^2.$$

By considering the whole range of error components with wavelengths from $\lambda/h = 2$ to ∞ it was shown in Wilkinson[6] (1970) that the optimum damping factor was bigger than that required to reduce the most unstable component to zero, and applying the same reasoning to this case gives the optimum factor as

$$f' = \frac{1}{1 - \frac{5}{96}k_{\min}(1 - M_{\text{rel}}^2)\cos^2\beta A^2}. \tag{38}$$

The convergence limit factor can be derived from (37) as

$$f_c = \frac{2}{1 - \frac{5}{48}k_{\min}(1 - M_{\text{rel}}^2)\cos^2\beta A^2}, \tag{39}$$

but use of f' from (38) will always ensure convergence since $f' < f_c$.

Equation (38) is the same as equation (35.33) of Wilkinson[6] (1970) except for the extra $\cos^2\beta$ term. However, compared to a set of q-o's normal to the flow A is $\sec^2\beta$ times as large, so the second term of the denominator is $\sec^2\beta$ times as big and f' is smaller. This shows that having q-o's inclined to the flow is less stable than having them normal to it.

The neglect of the first term on the right hand side in equation (36) is not without consequences for compressible flow since V_m will vary with β. An error component in streamline position will cause equal and opposite changes in V_m at $i = -1$ and $+1$, the amount depending on β and M_{rel}. The quantity dV_m/dm will then no longer be zero, but the whole term $r^2(d\theta/dm)(dV_m/dm)$ will have the same sign as the second term and add to it, making the iteration process less stable. This is only significant for high Mach Numbers and high deflections, and rather than complicate equation (39) with more terms, it has been found empirically to be sufficient to damp the change in slope, $d\theta/dm$ between iterations by the additional factor 0·5. This has worked well for the cases tried so far but if other cases cause difficulty then further investigation of this term may be necessary.

The number of iterations required is a function only of the damping factor f' as in the two-dimensional case, Wilkinson[6], (1970). To reduce the velocity error to ε times its initial value

$$\text{ITS} = \frac{\ln \varepsilon}{\ln(1 - f')}$$

or, for $\varepsilon = 1\%$

$$\text{ITS} = \frac{-4{\cdot}61}{\ln(1 - f')}. \tag{40}$$

2.4. Stagnation Streamline Shapes

The main reason for having tangential rather than 'normal' q-o's becomes apparent when considering the stagnation streamline shapes. Corresponding points on the suction and pressure surface s.s.l.'s at the same meridional station are at the ends of the q-o's. The shape of the s.s.l.'s can readily be changed by adding an amount δ_j to all of the θ ordinates on q-o'j. Considering an initial s.s.l. shape the calculation

method described above enables all of the velocities in the channel defined by the blades and s.s.l.'s to be found. For q-o's outside the blade row it is then necessary to find a set of increments δ_j to correct $(W_{i,N} - W_{i,1})$ to zero.

At q-o'i this is approximately equivalent to changing $\partial W/\partial\theta_{i,NM}$ by

$$\Delta\frac{\partial W}{\partial\theta_{i,NM}} = -\frac{(W_{i,N} - W_{i,1})}{(\theta_{i,N} - \theta_{i,1})}. \tag{41}$$

Equation (19) gives

$$\frac{\partial W}{\partial\theta_{i,NM}} = \cos\beta_{i,NM}\left\{\frac{d(V_m r^2)}{dm}\frac{d\theta}{dm} + V_m r^2\frac{d^2\theta}{dm^2} + 2\omega r\frac{dr}{dm}\right\}_{i,NM}.$$

This will be differentiated to find the effect of a change δ_j in the θ values at q-o'j.

$$\frac{\partial}{\partial\delta_j}\left(\frac{\partial W}{\partial\theta_{i,NM}}\right) = \frac{\partial\cos\beta_{i,NM}}{\partial\delta_j}\{\ldots\} + \cos\beta_{i,NM}\left\{\frac{d(V_m r^2)}{dm}\frac{\partial}{\partial\delta_j}\left(\frac{d\theta}{dm_{i,NM}}\right) + V_m r^2\frac{\partial}{\partial\delta_j}\left(\frac{d^2\theta}{dm_{i,NM}^2}\right)\right\} \tag{42}$$

$$\frac{\partial\cos\beta_{i,NM}}{\partial\delta_j} = -\sin\beta_{i,NM}\frac{\partial\beta_{i,NM}}{\partial\delta_j}.$$

But $\beta = \tan^{-1}\tan\beta$ and $\tan\beta = r(d\theta/dm)$, therefore

$$\frac{\partial\beta}{\partial\delta_j} = \frac{1}{1+\tan^2\beta}\frac{\partial\tan\beta}{\partial\delta_j} = \cos^2\beta r\frac{\partial}{\partial\delta_j}\left(\frac{d\theta}{dm}\right).$$

Therefore

$$\frac{\partial\cos\beta_{i,NM}}{\partial\delta_j} = \left\{-\sin\beta\cos^2\beta r\frac{\partial}{\partial\delta_j}\left(\frac{d\theta}{dm}\right)\right\}_{i,NM}$$

and equation (42) becomes

$$\frac{\partial}{\partial\delta_j}\left(\frac{\partial W}{\partial\theta_{i,NM}}\right) = \left[\cos\beta\left\{\left(-\sin\beta r\frac{\partial W}{\partial\theta} + \frac{d(V_m r^2)}{dm}\right)\frac{\partial}{\partial\delta_j}\left(\frac{d\theta}{dm}\right) + V_m r^2\frac{\partial}{\partial\delta_j}\left(\frac{d^2\theta}{dm^2}\right)\right\}\right]_{i,NM} \tag{43}$$

From the numerical differentiation formulae given in Section 2.5 the general form for $d\theta/dm$ is

$$\frac{d\theta}{dm_i} = \frac{1}{h_i}\sum_j k_{i,j}\theta_j.$$

Therefore

$$\left.\begin{aligned}\frac{\partial}{\partial\delta_j}\left(\frac{d\theta}{dm_i}\right) &= \frac{k_{i,j}}{h_i}\\ \text{similarly}\qquad\\ \frac{\partial}{\partial\delta_j}\left(\frac{d^2\theta}{dm_j^2}\right) &= \frac{l_{i,j}}{h_i^2}.\end{aligned}\right\} \tag{44}$$

The condition of periodicity at q-o'i then becomes

$$\sum_j \delta_j \cdot \frac{\partial}{\partial \delta_j}\left(\frac{\partial W}{\partial \theta}\right)_i = \frac{(W_{i,1} - W_{i,N})}{(\theta_{i,N} - \theta_{i,1})} \tag{45}$$

and from equations (43), (44) and (45)

$$\sum_j (A_i k_{i,j} + l_{i,j}) \cdot \delta_j = \frac{h_i^2}{r_i^2(\theta_{i,N} - \theta_{i,1})} \cdot \frac{(W_{i,1} - W_{i,N})}{V_{mi} \cos \beta_i} \tag{46}$$

where

$$A_i = \frac{h_i}{r_i^2} \cdot \frac{1}{V_{mi}}\left(-\sin \beta \cdot r \cdot \frac{\partial W}{\partial \theta} + \frac{d(r^2 V_m)}{dm}\right)_i . \tag{47}$$

Equation (43) has been non-dimensionalised to give equation (46) so that the coefficients and right hand side are of order 1·0 to avoid any possible inaccuracies in solving the equations.

Figure 3 shows the values of i and j for the leading and trailing edge s.s.l.'s. The choice of positions for the quasi-orthogonals will be discussed in Section 2.5.

Considering first the leading edge s.s.l. the unknowns are the δ_j for $j = 1$ to ML, where ML is in front of the leading edge. Equation (46) must be satisfied for q-o's 2 to ML, but at point 1 not only is $d^2\theta/dm^2$ very difficult to find accurately but in any case it is necessary to satisfy the condition of a specified inflow angle. Assuming that the current slope is $(r\, d\theta/dm)_1$ and that the required slope is $\tan \beta_1$, then, using a parabola through 3 points,

$$\frac{r_1}{h_1}(-1{\cdot}5\delta_1 + 2\delta_2 - 0{\cdot}5\delta_3) = \tan \beta_1 - r_1 \frac{d\theta}{dm_1}$$

or

$$-1{\cdot}5\delta_1 + 2\delta_2 - 0{\cdot}5\delta_3 = \frac{h_1}{r} \tan \beta_1 - h_1 \frac{d\theta}{dm_1}. \tag{48}$$

Equations (48) for $i = 1$ and (46) for $i = 2$ to ML give ML simultaneous linear equations for the q-o's shifts δ_j at $j = 1$ to ML. The equations are solved to give the new streamline shape.

For the trailing edge s.s.l. the unknowns are the δ_j for $j = MT + 1$ to M. Point MT is at the trailing edge and so cannot move. Equation (46) can be applied as it stands to the q-o's $i = MT + 1$ to $M - 1$. For q-o' M the curvature $d^2\theta/dm^2$ would again be difficult to find accurately but in any case the remaining equation is used to introduce a trailing edge loading condition. There is therefore no equation for the q-o'M, although δ_M is found by solving for the periodicity condition at the other points and serves to determine the outlet angle. At the trailing edge, $i = MT$, equation (45) could be applied directly and would correspond to equal velocities on a tangential line at the trailing edge. A more general condition may be just as easily applied however in which equal velocities occur on a line making an angle ϕ to the tangential direction, Fig. 4 where ϕ may be any specified value.

In Fig. 4 the velocities at points A and B may be written approximately in terms of the velocities at points on neighbouring q-o's and of the geometry. Assuming that the suction and pressure surfaces are nearly parallel to the trailing edge,

$$\Delta s \simeq \left\{ r \frac{\theta_t}{2} \cos \beta (\tan \beta - \tan(\beta - \phi)) \right\}_{MT} . \tag{49}$$

Approximating to velocities near $i = MT$,

$$W_A \simeq W_{MT,1} + \Delta s \frac{\partial W_{MT,1}}{\partial s} + \frac{\Delta s^2}{2} \frac{\partial^2 W_{MT,1}}{\partial s^2}$$

and

$$W_B = W_{MT,N} - \Delta s \frac{\partial W_{MT,N}}{\partial s} + \frac{\Delta s^2}{2} \frac{\partial^2 W_{MT,N}}{\partial s^2}$$

and putting

$$\frac{\partial W_{MT,1}}{\partial s} = \frac{1}{2h}(W_{MT+1,1} - W_{MT-1,1}),$$

$$\frac{\partial^2 W_{MT,1}}{\partial s^2} = \frac{1}{h^2}(W_{MT-1,1} - 2W_{MT,1} + W_{MT+1,1})$$

etc., and equating velocities at points A and B, requires

$$(W_{MT,N} - W_{MT,1}) = \left\{(W_{MT+1,N} - W_{MT-1,N} + W_{MT+1,1} - W_{MT-1,1}) \cdot \frac{\Delta s}{2h}\right.$$

$$\left. + (W_{MT+1,1} + W_{MT-1,1} - W_{MT+1,N} - W_{MT-1,N}) \cdot \frac{\Delta s^2}{2h^2}\right\} \Big/ \left(1 - \frac{\Delta s^2}{h^2}\right) \tag{50}$$

The existing value of $(W_{MT,N} - W_{MT,1})$ will usually differ from this and equation (50) can be used to find the correction required

$$\frac{\Delta \partial W}{\partial \theta_{MT}} = \frac{\Delta(W_{MT,N} - W_{MT,1})}{(\theta_{MT,N} - \theta_{MT,1})}$$

and this forms the right hand side of equation (45) for the trailing edge q-o.

The choice of a trailing edge condition has been the subject of much discussion but in reality it presents little problem either conceptually or numerically. It is shown in Chapter 5 of Thwaites[9] (1960) that for viscous flows, either attached or separated the steady lift condition involves the shedding of equal and opposite amounts of vorticity into the wake from the separation points on the suction and pressure surfaces. This implies equal velocities at the edges of the boundary layers at the separation points on the two surfaces. For a rounded or blunt trailing edge the condition, Fig. 4

$$W_A = W_B \tag{51}$$

which was used to give equation (50) is equivalent to specifying the separation point positions on the two surfaces. For a blunt trailing edge chamfered off at an angle, the corners seem obvious separation points, and this is very useful for dealing with the common steam turbine practice of chamfering off tangentially so that $\phi = 0$. For rounded trailing edges it is probably more reasonable to put $\phi = \beta_2$, making the line joining A and B normal to the mean line. However it is encouraging to find that the value of ϕ chosen is not at all critical. In Figs. 8 and 9 for a blade with a fairly thick rounded trailing edge and a highly curved camber line near the trailing edge, varying ϕ from 0 to 60 degrees caused the theoretical outlet angle to change only from 51·8 to 52·5 degrees. This might be compared with an outlet angle from the exact solutions for this section of 51·0 degrees with a rear stagnation point specified at a point at which

the tangent to the surface makes an angle to about 35 degrees to the θ-direction. However this implies that the stagnation streamline has an angle of 35 degrees to the axial giving a kink in the flow direction and less load near the trailing edge than with either of the streamline curvature cases so it is not strictly comparable. Nevertheless the agreement is still fairly close and the insensitivity of the outlet angle to ϕ has been shown. A number of other comparisons for turbine cases with experiment in Figs. 10–17 show very good agreement confirming the soundness of this approach. Because of its physical basis the assumption (51), leading to equation (50), may be expected to work for blunt trailing edges cut off at any angle, and for rounded or sharp trailing edges.

Summarising then for the trailing edge s.s.l. there are $M - MT - 1$ equations (46) for $i = MT + 1$ to $M - 1$, and one equation (46) with the right hand side derived from equation (50) instead of (41) for $i = MT$. These are solved for the $MT - M$ unknowns $\delta_j, j = MT + 1$ to M, to give the new trailing edge s.s.l. shape.

It is found with both leading edge and trailing edge s.s.l.'s that the rate of convergence is improved if the calculated shifts δ_j are multiplied by about 1·5. It is however found at high Mach Numbers that very small errors in slope, which occur until the s.s.l.'s reach their final positions, can restrict the flow area and cause spurious choking. It is better to slow the movement of the s.s.l.'s down to avoid this and this is done in the program by factoring the calculated δ_j's by

$$1{\cdot}5\sqrt{1 - M^2_{\text{rel},1,NM}}$$

for the leading edge s.s.l. and by

$$1{\cdot}5\sqrt{1 - M^2_{\text{rel},M,NM}}$$

for the trailing edge s.s.l.

One further point of importance concerns when the streamlines should be shifted during the course of the calculation. There are two iteration loops, the inner one of which corrects the solution of the equations of motion for given s.s.l. shapes and the outer one of which corrects the s.s.l. shapes. The inner loop has an accuracy tolerance specified in the input data of $\Delta W/\overline{W} = \varepsilon$ say. It is obviously not worth doing all of the iterations required to get the error down to ε with the initial incorrect s.s.l. shapes, so a lesser accuracy is in fact required for the early s.s.l. positions until the streamlines approach their final shapes. On the other hand if the solution for given s.s.l. shapes has errors that are too large, the correction to the s.s.l. shapes will contain a significant component due to the remaining numerical errors in the solution and the convergence of the s.s.l. shapes may be reduced. Without having done an exhaustive investigation of this, a reasonable compromise was taken to be to use a tolerance which is ε factored by a function of the number of streamline shifts, varying from 5ε for the initial s.s.l. shape and reducing to ε after about 10 s.s.l. shifts. The function used is

$$\varepsilon_p = \varepsilon\left(0{\cdot}627 + \frac{4{\cdot}373}{p+1}\right) \tag{52}$$

where p is the number of stagnation streamline shifts. A plot of $\varepsilon_p/\varepsilon \sim p$ is shown in Fig. 5.

2.5. Numerical Differentiation and Smoothing

It is necessary in evaluating the right hand side of equation (19) for $\partial W/\partial\theta$ to calculate $d(V_m r^2)/dm$, $d\theta/dm$, dr/dm and $d^2\theta/dm^2$ where the quantities $V_m r^2$, θ and r are known at points on the q-o's at unequal intervals of m. It is perhaps not always appreciated that since this is the only information the program has about the curves any numerical differentiation method will introduce smoothing. It was shown in Wilkinson[6] (1970) that if a trigonometrical interpolation method is used to fit a general curve through a set of points which may be thought of as a sum of Fourier components of wavelengths λ, then the accuracy of the numerical approximation to the derivatives of the Fourier components will be a function of λ/h, where h is the point spacing. In particular at high λ/h most methods are accurate but as λ/h reduces there is

at some stage a rapid fall in accuracy and at $\lambda/h = 2$ or less no methods are really adequate. A decision to use a particular number of points to define a curve, such as a blade surface shape, therefore implies that the shape does not require the presence of Fourier components with λ less than about 2 or 3 times h. In fact it may be decided that the minimum significant wavelength is more than 2 or 3 times h and the unwanted contributions to the derivatives at these wavelengths, due to small errors in input coordinates say, may need to be suppressed by further smoothing. The smoothing and differentiation formulae may be combined to give a single differentiation method of the form

$$\left.\begin{aligned} \frac{dy}{dx} &= \frac{1}{h}\sum_{n=-N}^{N} f_n y_n \\ \text{and} \\ \frac{d^2y}{dx^2} &= \frac{1}{h^2}\sum_{n=-N}^{N} g_n y_n. \end{aligned}\right\} \tag{53}$$

The correct choice of the coefficients f_n and g_n is therefore governed by the number of points to be used on the blade, usually about 15 for the cases considered so far, and by the minimum λ needed to define the blade shape. These give a minimum significant λ/h from which a suitable differentiation method can be chosen on the basis of the $(\lambda/h)_{10}$ values given in Wilkinson[6] (1970).

In order to give a rather more flexible formula than was possible with the examples in Wilkinson[6] (1970), a general smoothing process was introduced. The formulae for equal intervals of the argument will be considered first. For a quartic through 5 points

$$\frac{d^2y}{dx_0^2} = \frac{1}{12h^2}(-y_{-2} + 16y_{-1} - 30y_0 + 16y_1 - y_2). \tag{54}$$

This has $k_{\min} = -5{\cdot}33$ and $(\lambda/h)_{10} = 3{\cdot}35$. A common smoothing process replaces y_0 by the ordinate of the least squares parabola through 5 points. This is equivalent to

$$y_0 := \tfrac{1}{12}(-y_{-2} + 4y_{-1} + 6y_0 + 4y_1 - y_2) \tag{55}$$

where $:=$ means 'is replaced by' and the y's may be dy/dx, d^2y/dx^2 or any other quantity to be smoothed. Considering the $\lambda/h = 2$ component with $y_0 = 1$, $y_1 = y_{-1} = -1$, $y_2 = y_{-2} = 1$, etc., equation (55) gives $y_0 := -\frac{1}{3}$ a change of $-\frac{4}{3}$. A formula with no smoothing can be written as

$$y_0 := (\ldots 0xy_{-2} + 0xy_{-1} + 1xy_0 + 0xy_1 + 0xy_2 \ldots) \tag{56}$$

and any linear combination of equations (55) and (56) represents a smoothing process. Putting $y_0 := py_0$ for a range of p gives the formulae in Table 1.

Method	p	n	s_n -2	-1	0
A	1		(0	0	1
B	$\frac{2}{3}$	$\frac{1}{48}$	(−1	4	42
C	$\frac{1}{2}$	$\frac{1}{32}$	(−1	4	26
D	$\frac{1}{3}$	$\frac{1}{24}$	(−1	4	18
E	$\frac{1}{4}$	$\frac{1}{64}$	(−3	12	46
F	0	$\frac{1}{16}$	(−1	4	10
G	$-\frac{1}{3}$	$\frac{1}{12}$	(−1	4	6

These coefficients may be used in the form

$$y_0 := \sum_{n=-N}^{N} s_n y_n \tag{57}$$

when applied to sine curves of a range of λ/h they reduce the amplitude of the $\lambda/h = 2$ component to p times its original value and leave the $\lambda/h = \infty$ component unchanged, with intermediate values of λ/h having an amount of smoothing between p and 1, Fig. 6. If method F, with $p = 0$, is applied to equation (54) the expression

$$\frac{d^2y}{dx_0^2} = \frac{1}{h^2}(0{\cdot}00694y_{-4} - 0{\cdot}11111y_{-3} + 0{\cdot}44444y_{-2} + 0{\cdot}11111y_{-1} - 0{\cdot}90278y_0 + \ldots) \tag{58}$$

is produced which is the same as method 6 of Wilkinson[6] (1970) where it was obtained by 'double differentiation'. This shows that a continuous progression between the methods of Wilkinson[6] (1970) can be obtained by interpolating in the smoothing process.

A quite general 5 point smoothing formula can be derived without reference to least squares parabolas by noting that there are 3 coefficients involved and so any 3 reasonable conditions will determine them. One of these is that for $\lambda/h = \infty$ the process leaves the curve unchanged or, with

$$y_0 := ay_{-2} + by_{-1} + cy_0 + by_1 + ay_2 \tag{59}$$

then

$$2a + 2b + c = 1.$$

If we also specify

$$y_0 := py_0 \qquad \text{for} \qquad \lambda/h = 2$$

then

$$2a - 2b + c = p$$

and

$$b = \frac{1-p}{4}$$

and the third condition could be

$$y_0 := q \quad \text{at} \quad \lambda/h = 3 \quad \text{say,}$$

$$-a - b + c = q.$$

Therefore

$$c = \frac{1+2q}{3},$$

$$b = \frac{1-p}{4} \tag{60}$$

and

$$a = \frac{1-q}{3} - \frac{1-p}{4}.$$

Not all combinations of p and q are equally suitable and a curve of y_0/y_0 orig $\sim \lambda/h$ over the range from 2 to ∞ should be calculated to avoid going above 1 or below zero.

The choice of a particular amount of smoothing is a compromise between the loss of accuracy involved with too much and the reduction in $|k_{\min}|$ and hence in the number of iterations required, equations (40) and (38). Experience with about 15 q-o's on the blade, and of blade shapes typical of steam turbine applications, has shown that it is reasonable to use a smoothing formula equation (57) with $p = 0{\cdot}25$ and $q = 0{\cdot}443$, giving, from (60)

$$y_0 := -0{\cdot}00174y_{-2} + 0{\cdot}1875y_{-1} + 0{\cdot}62847y_0 + \ldots. \tag{61}$$

This expression is also shown in Fig. 6. When combined with equation (54) it gives $k_{\min} = -1{\cdot}66$ and $(\lambda/h)_{10} = 8{\cdot}2$. The argument for having these particular values of p and q is as follows. p is small but greater than zero. If p equals zero then the analysis works perfectly well for finding the flow with given stagnation stream line (s.s.l.) shapes but the simultaneous equations cf. (46), for finding δ_j become unsatisfactory. The values of $l_{i,j}$ in (46) are then the coefficients in equation (58). It is simpler to think of the equivalent formula for parabolas with double differentiation.

$$\frac{d^2y}{dx_0^2} = \frac{1}{h^2}(0{\cdot}25y_{-2} + 0y_{-1} - 0{\cdot}5y_0 + 0y_1 + 0{\cdot}25y_2). \tag{62}$$

This may easily be seen to split the points into two sets of odd and even numbered q-o's which do not affect each other through this equation. It is only at the end of the range at point $M - 1$ where a different formula has to be used that y_0'' is affected by y_{-1} or y_{+1}. This connection is not however strong enough to prevent the solution of equation (46) from producing two fairly independent sets of δ_j with consequently a large $\lambda/h = 2$ component in the shape and a large error in outlet angle. Also, as the formulae (58) or (62) cannot 'see' $\lambda/h = 2$ component the waviness is not corrected out at the next streamline shift. Putting $p = \frac{1}{4}$ seems sufficient to prevent this phenomenon and ensure smooth stagnation streamlines. It is of course possible to use one formula for the flow solution and another to give $k_{i,j}$ and $l_{i,j}$ for the s.s.l. shape solution but this was found to give a final solution in which periodicity was not quite achieved and could not apparently be made as accurate as required, however many streamline shifts were done.

For $p = \frac{1}{4}$, $k_{\min}$ occurs at about $\lambda/h = 3$ instead of 2 and is therefore proportional to q. Reducing q makes $k_{\min}$ less negative but increases $(\lambda/h)_{10}$. The value $q = 0{\cdot}443$ with $(\lambda/h)_{10} = 8{\cdot}2$ gives good results and no improvement was obtained with a higher q, although more iterations were of course required. If more complex blade shapes than those tried so far are encountered then it would be easy enough to increase q and calculate new values for the coefficients and $k_{\min}$.

This program is at a fairly early stage in its development and the recommended numerical methods may well be changed in detail as time goes on.

In order to find $k_{i,j}$ and $l_{i,j}$ in equations (44) and (46), equation (61) was applied to (54) giving

$$\frac{d^2y}{dx_0^2} = \frac{1}{h^2}(0{\cdot}00014y_{-4} - 0{\cdot}01794y_{-3} + 0{\cdot}20198y_{-2} + 0{\cdot}35127y_{-1} - 1{\cdot}07090y_0 + \ldots)$$

and to avoid having too many special end-of-range cases this was approximated by

$$\frac{d^2y}{dx_0^2} \simeq \frac{1}{h^2}(0{\cdot}20212y_{-2} + 0{\cdot}33333y_{-1} - 1{\cdot}07090y_0 + \ldots), \tag{63}$$

changing the coefficients so that k at $\lambda/h = 2$ remained the same. In the main program the smoothing process, (61) was applied as a sub-routine to both first and second derivatives after they had been calculated from equations (64) below and (54),

$$\frac{dy}{dx_0} = \frac{1}{12h}(y_{-2} - 8y_{-1} + 8y_1 - y_2) \tag{64}$$

which, after smoothing becomes

$$\frac{dy}{dx^0} = \frac{1}{h}(-0{\cdot}00014y_{-4} + 0{\cdot}01678y_{-3} - 0{\cdot}07263y_{-2} - 0{\cdot}40452y_{-1}\ldots)$$

$$\simeq \frac{1}{h}(-0{\cdot}04774y_{-2} - 0{\cdot}40452y_{-1}\ldots), \tag{65}$$

changing the coefficients so that the slope of a straight line was still correct.

At the end of the range, for dy/dx

$$\frac{dy}{dx_1} = \frac{1}{h}(-1{\cdot}5y_1 + 2y_2 - 0{\cdot}5y_3)$$

and

$$\frac{dy}{dx_2} = \frac{1}{h}(-0{\cdot}5y_1 + 0{\cdot}5y_3), \tag{66}$$

$(dy/dx)i$, $i = 3, 4, \ldots$ is given by (64). Then $(dy/dx)_2$ was smoothed by

$$y_2 := 0{\cdot}25y_1 + 0{\cdot}5y_2 + 0{\cdot}25y_3, \tag{67}$$

giving

$$\frac{dy}{dx_2} = \frac{1}{h}(-0{\cdot}60417y_1 + 0{\cdot}33333y_2 + 0{\cdot}125y_3 + 0{\cdot}16667y_4 - 0{\cdot}02083y_5). \tag{68}$$

For d^2y/dx^2,

$$\frac{d^2y}{dx_1^2} = \frac{d^2y}{dx_2^2} = \frac{1}{h^2}(y_1 - 2y_2 + y_3) \tag{69}$$

$(d^2y/dx^2)i$, $i = 3, 4, \ldots$ was given by (54). Then, applying (67) to these

$$\frac{d^2y}{dx_2^2} = \frac{1}{h^2}(0{\cdot}72917y_1 - 1{\cdot}1666y_2 + 0{\cdot}125y_3 + 0{\cdot}33333y_4 - 0{\cdot}02083y_5). \tag{70}$$

Analogous expressions for dy/dx_{M-1}, d^2y/dx_{M-1}^2 can readily be derived from (69) and (70).

Summarising then, derivatives in the main programs are found by equations (64) and (54) with end-of-range values by (66) and (69) and these are then both smoothed by equation (61) with (67) for end of range values. The $i = 1$ and M values are not smoothed. For finding the s.s.l. shapes with equation (46), the $k_{i,j}$ and $l_{i,j}$ values come from equations (65) and (63) with end-of-range values from (68) and (70).

Since the q-o's are generally at unequal intervals of m some modification to this procedure is necessary, and this also involves the choice of the best positions for the q-o's. In Section 2.4 and Fig. 3 one q-o was taken to be at the trailing edge, $i = MT$ and one just in front of the leading edge. Equations (38) and (40) show that for roughly equal rates of convergence on all parts of the blade $A \cos \beta = [r(\theta_N - \theta_1)]/h \cos \beta$ should be constant or, since $\theta_N - \theta_1$ is fairly constant $h/r = \Delta\xi$ should be proportional to $\cos \beta$. But this corresponds approximately to equal spacing along the mean line, Fig. 3, and this forms a simple rule for finding a reasonable q-o distribution. It is best to have the actual leading edge half way between two q-o's so the mean line length is measured in the (m, θ), or (ξ, θ) plane and divided by $\{MT - M - \frac{1}{2}\}$ to give the q-o spacing along the mean line. This q-o spacing is continued along the upstream and downstream s.s.l.'s usually with a gradual increase going away from the blade. The s.s.l.'s will usually fair into the mean line curve unless a very 'off-design' incidence is being considered and so m_i will usually be a smooth function of q-o number i. It is then possible to use the equal interval formulae for derivatives above by using 'parametric differentiation' Wilkinson[6] (1970).

$$\frac{dy}{dm} = \frac{dy/di}{dm/di}$$

and

$$\frac{d^2y}{dm^2} = \frac{\dfrac{dm}{di}\dfrac{d^2y}{di^2} - \dfrac{dy}{di}\cdot\dfrac{d^2m}{di^2}}{(dm/di)^3}. \tag{71}$$

However, to avoid errors due to lack of smoothness in $m \sim i$, particularly in finding d^2y/dm^2, the input coordinates z_i, r_i, $\theta_{i,1}\theta_{ti}$, and Δr_i are all smoothed twice with respect to i using equation (55). This reduces discrete errors to $\frac{1}{4}$ of their input values and $\lambda/h = 2$ components to $\frac{1}{9}$th. It is necessary to prevent the kink in the s.s.l. at leading edge and trailing edge from affecting the section shape during the smoothing process, so the values of the coordinate being smoothed are maintained unchanged at $i = ML + 1$ and $ML + 2$ and at $i = MT - 1$ and MT. This preserves the shape of the blade at leading and trailing edges. At input the tangential thickness coordinate θ_t is put equal to zero on the leading and trailing s.s.l.'s and suddenly increases to or decreases from a non-zero value at leading and trailing edges. The smoothing process will however introduce non zero values in the form of a small cusp at each end of the blade. The cusps carry no load, as the periodicity condition ensures equal velocities each side of them, and merely serve to divide the flow.

There is no particular necessity for θ_t to be zero on the s.s.l.'s and if it was desired to represent a thick wake, a non-zero value of θ_t behind the trailing edge would do this. As programmed such a wake would have zero load on it in the tangential direction. The program could easily be modified to have zero load normal to the wake or to have a normal load which was a function of an input wake momentum and of the calculated wake curvature, the wake development and curvature being calculated as part of the program.

A fundamental limitation with streamline curvature methods is their inability to give an accurate potential flow solution in the leading and trailing edge regions, where there is a right-angled kink in the wall shape as the stagnation streamline meets the wall. In terms of a Fourier analysis of the streamline shape through the kink, all wavelengths down to $\lambda/h = 0$ would be needed for exact representation. With a finite number of q-o's in the kink region, there is never enough information present to fully define the shape and this manifests itself in the fact that all numerical differentiation methods neglect contributions from components with λ/h less than about 2. With smoothing, of course, even higher wavelength components are ignored. Some error in estimating curvatures, and hence velocity gradients, in the stagnation regions is therefore inevitable and a choice must be made in which improving the accuracy by having more q-o's and a more accurate differentiation method is traded against the reduced stability and hence greater number of iterations required for higher A and $|k_{min}|$. The introduction of a small cusp could easily be avoided but is thought to have a generally beneficial effect. The degree of error caused

by smoothing out the stagnation regions with the present numerical coefficients can be seen in Figs. 8 to 17. For steam turbine applications where flow near the leading edge of nozzles is not very important, and where impulse blades generally have thin leading edges, this degree of agreement is probably quite acceptable in the leading edge region. At the trailing edge the real flow is probably more like the smoothed out streamline curvature approximation, due to the boundary layers, wake and separations, than the idealised potential flow model with a stagnation point, and good agreement on loading and outlet angle is obtained. For compressor cascades or large off-design incidences a more accurate version of the program might be required and could easily be produced using the methods outlined above.

2.6. Starting Values

In order to start the calculation off, some initial values of parameters appearing on the right hand side of equation (19) must be specified. To find the overall velocity level a zero velocity gradient $\partial W/\partial\theta = 0$ is assumed and a flow angle $r(d\theta/dm)$ is required. An initial θ distribution is needed also for $d^2\theta/dm^2$ and it was at first thought that the streamlines could be spaced uniformly along the q-o's. This worked well enough at low Mach Numbers but not at higher mass flows where spurious choking was often predicted at, or just before, the trailing edge q-o. This was because the uniform spacing approximation results in a slope $d\theta/dm$ that is slightly too high near the trailing edge, with a consequent reduction in effective flow area. The Mach Number is so sensitive to area near $M = 1$ that this was often sufficient to cause choking to be indicated. The cure for this was to space the streamlines uniformly along normals to the flow and then interpolate back to find the positions along the q-o's. As this is not quite as straightforward as it sounds a brief description of the method will be given.

The mid-streamline for uniform spacing was found from

$$\theta_{i,NM} = (\theta_{i,1} + \theta_{i,N})/2$$

and differentiated to give $r_i(d\theta/dm_{i,NM}) = d\theta/d\xi_{i,NM}$. The normal through the point i, NM is then

$$\theta = a\xi + b$$

where

$$a = \frac{-1}{d\theta/d\xi_{i,NM}}$$

and

$$b = \theta_{i,NM} - a\xi_{NM}.$$

The intersections of this normal with the suction and pressure surface streamlines, $j = 1, N$, were then found. In Fig. 7 in the ξ, θ plane a set of quasi-normals are found, numbered from KF to KB where KF is found by

$$\xi_{KF} \geqslant \xi_1 + \frac{(\theta_{1,N} - \theta_{1,1})}{4} \sin 2|\beta_{1,NM}|,$$

where

$$\beta = \tan^{-1} r\frac{d\theta}{dm}.$$

Similarly KB follows from

$$\xi_{KB} \leqslant \xi_M - \frac{(\theta_{M,N} - \theta_{M,1})}{4} \sin 2|\beta_{M,NM}|.$$

For any q-n i, $KF \leqslant i \leqslant KB$, at intersection with the suction surface (or s.s.l.).

$$\xi'_{i,1} \simeq \xi_{i,NM} + \frac{(\theta_{i,N} - \theta_{i,1})}{4} \sin 2\beta_{i,NM}.$$

This locates the set of 4 points along the suction surface nearest to the intersection point, two either side of $\xi'_{i,1}$. The coefficients C_1 to C_4 of a cubic through these points are found, by solving simultaneous equations, as

$$\theta = C_1 + C_2\xi + C_3\xi^2 + C_4\xi^3.$$

Then, for equal θ at the intersection of the q-n and the cubic,

$$f(\xi) = (C_1 - b) + (C_2 - a)\xi + C_3\xi^2 + C_4\xi^3 = 0$$

and this is solved for the accurate $\xi'_{i,1}$, starting from the approximate $\xi'_{i,1}$ above, by Newton's method, and θ'_i, is found.

A similar procedure is used to find $\xi'_{i,N}$, $\theta'_{i,N}$ on the pressure surface (or s.s.l.). With the ends of the quasi-normal known, the intermediate streamline positions are found by linear interpolation for uniform spacing. This gives $\xi'_{i,j}$, $\theta'_{i,j}$ for $KF \leqslant i \leqslant KB$, $1 \leqslant j \leqslant N$ defining the uniformly spaced streamline positions on the quasi-normals. It is now necessary to interpolate back to find the corresponding $\theta_{i,j}$ values along the q-o's. For the triangular regions at either end of the channel the streamlines are still left spaced uniformly along the q-o's. These regions are defined by

$$\xi_i \leqslant \xi'_{KF,j}, \qquad j = 1 \text{ to } N$$

and

$$\xi_i \geqslant \xi'_{KB,j}, \qquad j = 1 \text{ to } N.$$

For points not in the triangular regions, for each (i, j) the set of 4 points $(\xi'_{i,j}, \theta'_{i,j})$ along the jth streamline is found such that 2 are either side of ξ_i and 4-point interpolation used to find $\theta_{i,j}$.

3. Data for Computer Program

A large drawing of one blade is required on which the initial shapes of the stagnation streamlines are drawn in. For a three-dimensional cascade it is probably best to draw the blade in the transformed (ξ, θ) plane. Selection of positions for the quasi-orthogonals was discussed in Section 2.5, and summarising this,

(a) One q-o should go through the mean line at the trailing edge.
(b) The leading edge should be half way between two q-o's.
(c) Divide up the mean line length between q-o's ML and MT with equally spaced q-o's.
(d) Continue this spacing for the q-o's along the stagnation streamlines, but with a gradual increase going away from the blade.
(e) The stagnation streamlines must extend sufficiently far up and downstream of the blade so that a region of substantially parallel uniform flow is reached.

(f) The total number of q-o's allowed, as programmed, is 30, but this could be increased if required. This means that 12 to 15 can be on the blade.

(g) At the trailing edge, Fig. 4, the point (MT, N) (or $(MT, 1)$) may be off the actual blade and it is necessary to draw in an approximate fairing line from the pressure surface to the s.s.l. as indicated and take the point as being on that.

Either two- or three-dimensional cascades may be input and are indicated by putting IDIM = 2 or 3. For IDIM = 2 the $\theta_{i,1}$ and θ_{ti} ordinates are input as dimensional quantities in inches and divided by the constant radius r_i within the program. For IDIM = 3 the $\theta_{i,1}$ and θ_{ti} values are in radians and are true angular coordinates.

The maximum number of streamlines allowed including suction, 1, and pressure N, surfaces is 9. This could be increased if required but 7 streamlines are usually sufficient.

N must be odd.

All data cards use input formats and these must be strictly observed.

The data required is set out as follows.

(2) Title

(Any characters from columns 2 to 66)

M N ML MT

(All format I5)

IDIM

(I2)

z_1 r_1 $\theta_{1,1}$ θ_{t1} Δr_1 ($z, r, \Delta r$ in inches. θ, θ_t in inches, IDIM = 2 or in radians IDIM = 3)

(All F10.3)

z_M r_M $\theta_{M,1}$ θ_{t_M} Δr_M

ϕ (degrees)

(F10.3)

(4) RPM γ TOL NB ITS JUMPS

(F10.3) (F10.3) (F10.3) (I5) (I5) (I5)

(1) V_{z_1} V_{θ_1} h_{t_1} p_{t_1} loss coeft.

(All F10.3)

NEXT (I2)

= 0, finished
= 1, new V_{z_1}, V_{θ_1}, etc., repeat from (1)
= 2, new geometry, repeat from (2)
= 3, new ϕ, give new ϕ value only
= 4, new RPM, γ, etc., repeat from (4)
(V_{z_1}, V_{θ_1} in ft/sec, h_{t_1} in Btu/lb, p_{t_1} in lb/in^2)

NB is the number of blades. For a two-dimensional case this must fit in with r to give the right pitch from

$$s = \frac{2\pi r}{\text{NB}}$$

or

$$r = \frac{s \,.\, \text{NB}}{2\pi} \text{ where } s \text{ is in inches.}$$

Any convenient values of NB and r may be used. Also any constant Δr may be used for the two-dimensional case.

For the three-dimensional case it is only the ratios of Δr from one q-o to another that matter and any convenient magnitude can be used.

TOL is the estimated remaining velocity error required, divided by the mean velocity, taking the maximum of this ratio for all q-o's. A value of 0·005 has been found reasonable.

ITS is the maximum number of iterations that will be done for any streamline shape and prevents the program running indefinitely if it does not converge for some reason. It can be found approximately from equation (40), otherwise a value of about 50 can be used.

JUMPS is the maximum number of stagnation streamline shifts that will be done, although the program will probably converge with less. About 15 shifts are usually enough.

V_{z_1} and V_{θ_1} with dr/dm, from the geometry, and the RPM and r_1, define the relative and absolute inlet angles and these will be preserved during the calculation. The inlet angle does not depend on the initial s.s.l. shape.

For a range of inlet mass flows or Mach Numbers it is advisable to start with the highest and work down to lower Mach Numbers. This is to take advantage of (a) the ability to space the trailing stagnation streamline well away from the back of the blade and (b) the initial streamline spacing, uniform normal to the flow, which is close to the correct spacing for sonic flow. Both of these things minimise the possibility of spurious choking being predicted, and simple sums based on passage areas should enable the critical mass flow to be estimated beforehand and avoided.

The streamline shifting method can cope with large changes in inlet angle and to change the incidence it is usually sufficient to put NEXT = 1 and change V_{z_1} and V_{θ_1} without having to change the whole geometry.

For dry steam a good approximation to its properties is obtained by using $\gamma = 1{\cdot}3$ and $(h_t - 835)$ instead of h_t. The calculated h_t values in the program output should then have 835 added to them.

The output includes values of all geometrical and flow parameters over the whole grid. The pressure coefficient S is one used by NASA and is

$$S_{i,j} = \frac{p_{t_1} - p_{i,j}}{\frac{1}{2}\rho_1 V_1^2} \tag{72}$$

where subscript 1 refers to q-o' 1.

The velocity ratio V/V_2 is also output and this is actually

$$\left(\frac{V}{V_2}\right)_{i,j} = \frac{W_{i,j}}{W_{M,NM}}.$$

Note that this non-dimensionalises relative to a velocity on the last q-o' and that, whilst this represents a mean trailing edge value in two-dimensions, it does not in three-dimensions because of change of radius and annulus area.

The program is in FORTRAN IV and on the IBM 360-75 run times with $M = 30$, $N = 7$ are about 0·4 secs per iteration, and 0·14 secs per streamline shift giving an overall run time of about 20 to 40 secs. With the IBM 360-85 run times are expected to be about 40 per cent of those on the -75, giving overall times of 8 to 16 secs. This is per case, and each Mach Number and incidence combination is a separate case, although for a range of these a new solution is derived from the previous one and the full time may not be required.

4. Comparisons with other Theories and with Experiment

The method should be applicable to a wide range of cases as it can deal with compressible or incompressible flow, changes of duct area in the flow direction, changes of radius and relative vorticity effects on rotating blades. It can therefore be used for axial, mixed flow, or radial flow turbines or compressors including steam turbines, gas turbines, axial and centrifugal compressors and gas circulators. A very extensive program of work would be needed to verify the method of all possible geometries in all these

applications and only a limited number of comparisons for cases relevant to steam turbines have been done so far. The particular cases considered are those with incompressible or compressible axial flow, for which exact or experimental results were available and with incompressible mixed flow with fixed and rotating blades for which almost exact solutions were available from the Wilkinson/Martensen singularity method Wilkinson[10,11] (1967), (1969).

Figures (8) and (9) show the 112 degrees camber cascade obtained by Gostelow[12] (1964) by transformation and a comparison between the associated exact solution and the streamline curvature solution. This has already been discussed towards the end of Section 2.4 where it was stated that the outlet angle in the s/lc. solution, with $\phi = 0$ would not be expected to be the same as the 'exact' value as the two Kutta–Joukowski conditions were not equivalent. If the s/lc. velocities, V/V_2, are factored by the ratio of the V_2's of the two solutions so that they are non-dimensionalised on the same value of V_2 the two velocity distributions are then in almost exact agreement except at the leading and trailing edges. Near the leading edge the smoothing out process, due to the inaccurate differentiation method and the introduction of a small cusp, has prevented the stagnation velocity from being obtained and caused a more gradual transition from the upstream to blade surface velocities. In the trailing edge region there has also been some smoothing out and the extra load due to the higher turning angle appears here. Apart from this there is generally very good agreement between the two methods.

Figures (10) and (11) show the blade shape and velocity distributions for a NASA section, Whitney[14] (1967). There is generally good agreement including the back of the blade where the Mach Number is fairly constant at about 0·85. The outlet angle predicted is 0·5 degrees too high and this may also be reflected in a tendency for the load to be too high near the trailing edge. It is likely that there were not quite enough q-o's after the blade, as completely uniform flow had not been established by the last one. There was still a small variation in tangential velocity and this may have affected the final result. Another possible explanation is that viscous effects, due to the suction surface boundary layer displacement thickness being larger than that on the pressure surface at the trailing edge, may have caused the 'effective' blade shape to turn the flow slightly less.

Figures (12) to (14) show some comparisons for compressible two-dimensional flow past a cascade of NACA primary series turbine blades Dunavant[13] (1956) at two incidences and Mach Numbers. The blade had $\theta_c = 80$ degrees and was at a stagger of 38·4 degrees. The coordinates can be found in Dunavant and Erwin[13] (1956).

In Fig. (12) some difficulty was caused by the experimental inlet and outlet Mach Numbers and flow angles not satisfying continuity for isentropic flow, as the s/lc. values must do. Addition of loss effects would make the discrepancy greater still. It may be that, due to the general increase in the flow velocity through the blade row, the side wall boundary layers have become thinner and this has reduced the outlet Mach Number. The experimental $\frac{1}{2}\rho_1 V_1^2 = (\gamma/2)p_1 M_1^2$ for a given M_2 would then be relatively larger than theory and S would be reduced. However, scaling by the ratio of the theoretical/experimental $\frac{1}{2}\rho_1 V_1^2$ values takes the theoretical S curve only about half-way towards the experimental values in Fig. 12. There must therefore be some other error. It must be noted that (a) for the given outlet Mach Number the theory satisfies continuity while the experiment does not, (b) the theory gives the experimental outlet angle to 0·1 degrees, (c) since the change in tangential momentum is reflected in the load on the blade the theoretical load must be correct, (d) the shapes of the theoretical and experimental $S \sim x/c$ curves are very similar. It is concluded that the experiment contains some unknown error in the non-dimensionalising quantity $\frac{1}{2}\rho_1 V_1^2$. A suitable value can easily be found to make the theoretical and experimental curves almost coincident.

This tendency for the theoretical S values to be higher than experimental ones is also shown in Figs. (13) and (14), although to a lesser extent the outlet Mach Numbers being rather different in the latter. The inlet and outlet Mach Numbers and angles from experiment are nearer to satisfying continuity but presumable $\frac{1}{2}\rho_1 V_1^2$ is still too high. The outlet angles are predicted very well and the shapes of the curves are in good agreement. There is a tendency for the theoretical curve to dip before the trailing edge on the suction surface, particularly in Fig. 14, which does not seem to appear very much in the experiment, although there are no pressure tappings over the last 10 per cent chord and S might actually rise toward the trailing edge. This might also be due to the higher theoretical outlet Mach Number.

In general, with some fairly reasonable scaling, the theoretical pressure distributions show good agreement with experiment and the outlet angles are predicted very well.

The comparisons so far all deal with axial flow, over a range of Mach Number. Three-dimensional flow effects have two main forms, change of annulus area and change of radius of the meridional stream surface, and either or both of these may be present. There are no exact solutions or test data on the compressible three-dimensional cascade case and the best available comparative predictions are those for incompressible flow from the Wilkinson/Martensen mixed flow analysis method Wilkinson[10,11] (1967), (1969). This method uses singularities to give an almost exact solution. A case was therefore run on both the streamline curvature and singularity methods for a section derived from, but not the same as, the NASA primary series turbine blade. The (z, r, θ) coordinates for points on the blade are given in Table 1. The meridional stream surface had 45 degrees flare and was defined by

$$r = 78{\cdot}6 + z$$

where the leading edge is at $z = 0$ and the axial chord is 7·86 ins giving a 10 per cent increase in radius from leading to trailing edge. The annulus area, defined by Δr also increases according to

$$\Delta r = \Delta r_{\text{l.e}}\left(1 + \frac{z}{39{\cdot}3}\right).$$

This corresponds to a hub/tip = 0·5 and conical meridional streamlines from an origin at $(-39{\cdot}3, 39{\cdot}3, \theta)$. The upstream and downstream limits of the region of interest were taken as $z = -4{\cdot}18$ to $+11{\cdot}53$ and a relative inlet angle of $\theta_1 = 10$ degrees was used at $z = -4{\cdot}18$ for both fixed and rotating blades. For the latter the rotational speed parameter, $\omega r_1/V_{m1}$, at $z = -4{\cdot}18$ was 1·0. The streamlines are not straight either upstream or downstream due to the changing radius and annulus area but θ_2 was the flow angle at $z = 11{\cdot}53$. A plot of the blade shapes and predicted streamlines is shown in Fig. 15 for the transformed plane (ξ, θ) in which all angles are preserved relative to the meridional stream surface. In this case where the flow was on a cone the surface could have been 'unwrapped' and plotted without distortion but this would not generally be so.

Also the z = constant lines would have been arcs of circles and it would not have been as easy to see the flow angles.

Figures (16) and (17) compare the predictions of the streamline curvature and the singularity methods for fixed and rotating blades. There is close agreement for velocity distributions and outlet angles in both cases, with the usual smoothing out error near the leading edge. There is a 30 per cent annulus area increase in both cases, so this large effect is evidently allowed for successfully and the relative vorticity effect can also be seen to be large by comparing the loadings in the two cases. Although only for one case, this does confirm that the program is including correctly the effects of annulus area and radius change for both fixed and rotating blades.

Taking this in conjunction with the earlier comparisons for compressible flow in axial cases it seems reasonable to conclude that the method works successfully for turbine cascades of the type illustrated for general three-dimensional compressible flow cases. It should also be applicable to a wide range of other cascades including axial, mixed and centrifugal compressors but further comparisons would be necessary to verify this.

5. A New Design Method

The design or 'inverse' problem, in its usual aerodynamic form, is to calculate the blade shape that will give a specified velocity distribution on one or both surfaces. The method developed in Section 2.4 for adjusting the stagnation streamline shapes to give a specified, zero difference between the velocities at the ends of a q-o', can readily be extended to obtain specified blade surface velocities.

Consider a case where the solution for the flow through the channel with the initial s.s.l.'s has attained sufficient accuracy to make it worthwhile shifting the s.s.l.'s to make them more periodic. We now consider shifts δ_j for all q-o's $j = 1$ to M. The periodicity condition for $i = 2$ to ML and $MT + 1$ to $M - 1$ is still equation (45) and that for $i = MT$ is found from equation (50). The $k_{i,j}$ and $l_{i,j}$ values now have to be calculated for δ_j's on the blade as well.

On the blade if the required suction surface velocities are $W'_{i,1}$, $i = ML + 1$ to $MT - 1$, then a change of $\partial W/\partial\theta$ on the mid-streamline is required given approximately by

$$\Delta\frac{\partial W}{\partial\theta_{i,NM}} \simeq \frac{-2(W'_{i,1} - W_{i,1})}{(\theta_{i,N} - \theta_{i,1})} \tag{73}$$

from which, by comparison with equation (41) a new right hand side for equation (46) can be found.

This gives $M - 1$ equations for the M unknown δ_j values, but in fact one of the δ_j's is not needed since a uniform translation due to adding δ to all q-o's will have no effect. Without loss of generality, therefore, one of the δ_j's at $j = 1$ or ML or MT, say, is set to zero and the remaining $M - 1$ equations solved to give the new blade and stagnation streamline shapes. This would replace the procedure for finding the s.s.l. shapes alone and, apart from the extra time needed to deal with about 30 simultaneous equations instead of about 7 before, the whole calculation should not take much longer than the analysis method.

This design method has not yet been programmed although it is a relatively simple modification to the existing program and could easily be done if there was a demand. The main drawback to the prescribed velocity distribution methods is that the outlet angle cannot be specified as well, but comes out as a derived quantity from the calculation. It would be necessary to try several velocity distributions of the desired type to find the one giving the right outlet angle, and this might be a useful 'light-pen' exercise. The other approach to designing blade shapes uses the fact that the outlet angle can be estimated fairly accurately from the opening/pitch rule, for turbines at least, and so it is possible to draw several different blades with the same outlet angle. The velocity distributions can be found by the analysis method and geometrical variations introduced to obtain the best design. The latter approach, which could also be done by light pen, is probably more satisfactory, although the P.V.D. method may be useful in some applications, or as a way of eliminating velocity peaks or adverse pressure gradients on sections that are nearly good enough.

6. Conclusions

6.1. A new method has been given for calculating the compressible flow through a three-dimensional cascade defined by the intersection of a meridional stream surface with a blade row. The effects of changing annulus area and radius for fixed and rotating blades are included. The streamline curvature technique is used with tangential quasi-orthogonals, and the upstream and downstream stagnation streamline shapes are determined iteratively to satisfy periodicity in the tangential direction. A Kutta–Joukowski condition suitable for thin and thick trailing edges is used to find the outlet angle.

6.2. The method has been shown to be in good agreement with other theories and with experiment for special cases and, by implication, should be applicable to a wide range of flow cases including axial, mixed and radial flow in turbines, compressors, fans, circulators and pumps from incompressible to choked flow.

6.3. A new design method has been suggested and outlined for finding the blade shape to give a prescribed suction surface velocity distribution for a given tangential thickness distribution. This should have the same range of application as the analysis method.

Acknowledgement

The Author would like to thank the Director of the Marchwood Engineering Laboratory of the Central Electricity Generating Board for permission to publish this report.

LIST OF SYMBOLS

A	Aspect ratio of streamline curvature grid element, equation (37)
$\bar{c}$	Compressibility function, equation (32)
f	Damping factor to correct initial error to zero, equation (37)
f'	Optimum damping factor, equation (38)
f_c	Convergence limit damping factor, equation (39)
f_n	Numerical differentiation coefficient, equation (53)
g	Gravitational acceleration
g_n	Numerical differentiation coefficient, equation (53)
h	Static enthalpy, or point spacing interval
h_t	Total enthalpy
I	Enthalpy function, equation (4)
J	Mechanical equivalent of heat
K	A constant
k	Numerical differentiation function, Wilkinson[6], (1970)
$k_{i,j}$	Numerical differentiation coefficient equation (44)
$l_{i,j}$	Numerical differentiation coefficient equation (44)
M	Mach Number, or mass flow, or number of quasi-orthogonals
m	Distance along meridional stream surface, equation (9)
$\overline{M}$	Factored mass flow, equation (27)
ML	No. of q-o' just in front of leading edge
MT	No. of q-o' through trailing edge
N	No. of streamlines
NB	No. of blades
NM	No. of mid-streamline
p	Pressure
q	Tangential distance measured from suction surface
r	Radial coordinate
Δr	Radial thickness increment between two meridional stream surfaces
S	Pressure coefficient, equation (72)
s	Entropy, or distance along streamline in meridional stream surface
s_n	Numerical smoothing coefficient, equation (57)
T	Absolute temperature
t	Time
V	Absolute velocity

W	Relative velocity
x, y	Cartesian coordinates
z	Axial coordinate
α	$\tan^{-1}(dr/dz)$, Fig. 1
β	$\tan^{-1} r(d\theta/dm)$, Fig. 1
γ	Ratio of specific heats
δ_j	Change in position, in θ-direction, of quasi-orthogonal j
θ	Tangential coordinate
θ'	Relative tangential coordinate
θ_t	Blade tangential thickness coordinate
λ	Wavelength of error component
ξ	Transformed meridional coordinate, equation (30)
ρ	Density
ϕ	Trailing edge cut-off angle, Fig. 4
$\psi, \bar{\psi}$	Stream function
ω	Angular velocity of blade row

Subscripts

1	Upstream, suction surface or first quasi-orthogonal
2	Downstream
M	Last quasi-orthogonal
m	In the meridional direction
N	On the pressure surface
NM	On the mid-streamline
r	In the radial direction, or relative to coordinate system moving with the blades
rel	Relative to coordinate system moving with the blades
t	total or stagnation value
z	In the axial direction
θ	In the tangential direction

REFERENCES

No.	Author(s)	Title, etc.
1	D. J. L. Smith and D. H. Frost	Calculation of the flow past turbomachine blades. I. Mech. E. Thermodynamics and Fluid Mechanics Convention, Paper 27 (1970).
2	W. Jansen	A method for calculating the flow in a centrifugal impeller, when entropy gradients are present. Unpublished N.R.E.C. report.
3	J. P. Bindon and A. D. Carmichael	Streamline curvature analysis of compressible and high Mach Number cascade flows. Proc. I. Mech. E (1970).
4	T. Katsanis	Use of arbitrary quasi-orthogonals for calculating flow distribution in the meridional plane of a turbomachine. NASA TN D-2546 (1964).
5	T. Katsanis	Use of arbitrary quasi-orthogonals for calculating flow distribution on a blade-to-blade surface in a turbomachine. NASA TN D-2809 (1965).
6	D. H. Wilkinson	Stability, convergence and accuracy of two-dimension streamline curvature methods using quasi-orthogonals. I. Mech. E. Thermodynamics and Fluid Mechanics Convention, Paper 35 (1970).
7	D. H. Wilkinson and K. Allsopp	The effect of duct height variation on the potential flow through a 2-D cascade. English Electric Co. Mechanical Engineering Laboratory. Tech. Memo. No. W/M(3F). u.9233 (1969).
8	D. H. Wilkinson	Streamline curvature methods for calculating the flow in turbomachines. English Electric Co. Mechanical Engineering Laboratory. Report No. W/M(3F) p.1591 (1969).
9	B. Thwaites (Ed.)	Incompressible Aerodynamics. Clarendon Press (1960).
10	D. H. Wilkinson	The calculation of rotational non-solenoidal flows past two-dimensional aerofoils and cascades. English Electric Co. Ltd. Mechanical Engineering Laboratory Report No. W/M(6c) p.1291 (1967).
11	D. H. Wilkinson	The analysis and design of blade shapes for radial, mixed and axial flow turbomachines with incompressible flow. English Electric Co. Mechanical Engineering Laboratory Report No. W/M(3F) p.1578 (1969).

12 J. P. Gostelow . . . . . Potential flow through cascades—a comparison between exact and approximate solutions.
ARC C.P.807 (1963)

13 J. C. Dunavant and J. R. Erwin . . . . Investigation of a related series of turbine-blade profiles in cascade.
NACA TN 3802.

14 W. J. Whitney, E. M. Szanca, T. P. Moffitt and D. E. Monroe Cold air investigation of a turbine for high-temperature-engine application.
NASA TN D-3751 (1967).

TABLE 1

Coordinates of modified NASA primary series blade used in 45° flare test case. Number of blades = 93, $\theta_1 = 10°$ (relative) $\omega r_1/V_{m_1} = 0, 1{\cdot}0$.

z	r	θ_{Suct}	θ_{Pres}	Δr
0	78·60	0·0182	0·0182	0·1000
0·330	78·93	0·0232	0·0155	0·1008
1·010	79·61	0·0252	0·0133	0·1026
1·688	80·29	0·0245	0·0107	0·1043
2·338	80·94	0·0219	0·0075	0·1060
2·947	81·55	0·0181	0·0034	0·1075
3·514	82·11	0·0134	−0·0012	0·1089
4·048	82·65	0·0079	−0·0062	0·1103
4·552	83·15	0·0020	−0·0112	0·1116
5·028	83·63	−0·0044	−0·0164	0·1128
5·480	84·08	−0·0112	−0·0217	0·1139
5·909	84·51	−0·0182	−0·0271	0·1150
6·330	84·93	−0·0257	−0·0326	0·1161
6·746	85·35	−0·0333	−0·0385	0·1171
7·140	85·74	−0·0406	−0·0443	0·1182
7·500	86·10	−0·0473	−0·0501	0·1191
7·860	86·46	−0·0541	−0·0562	0·1200

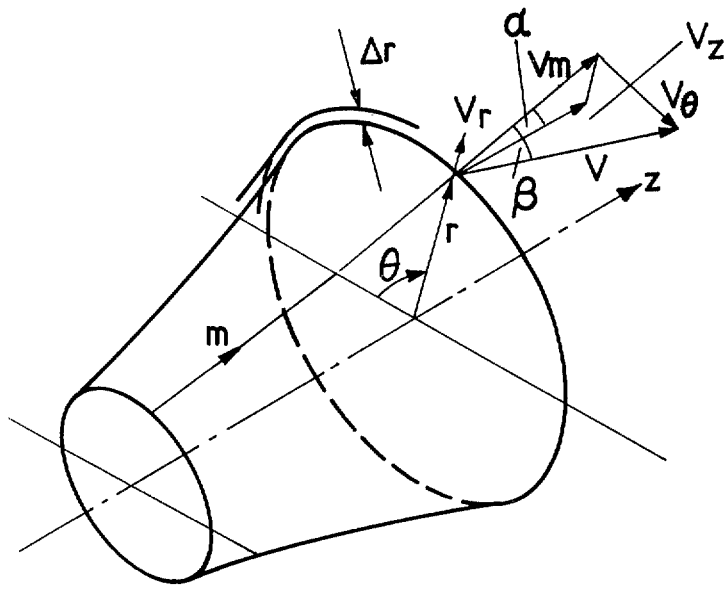

FIG. 1. Coordinate system.

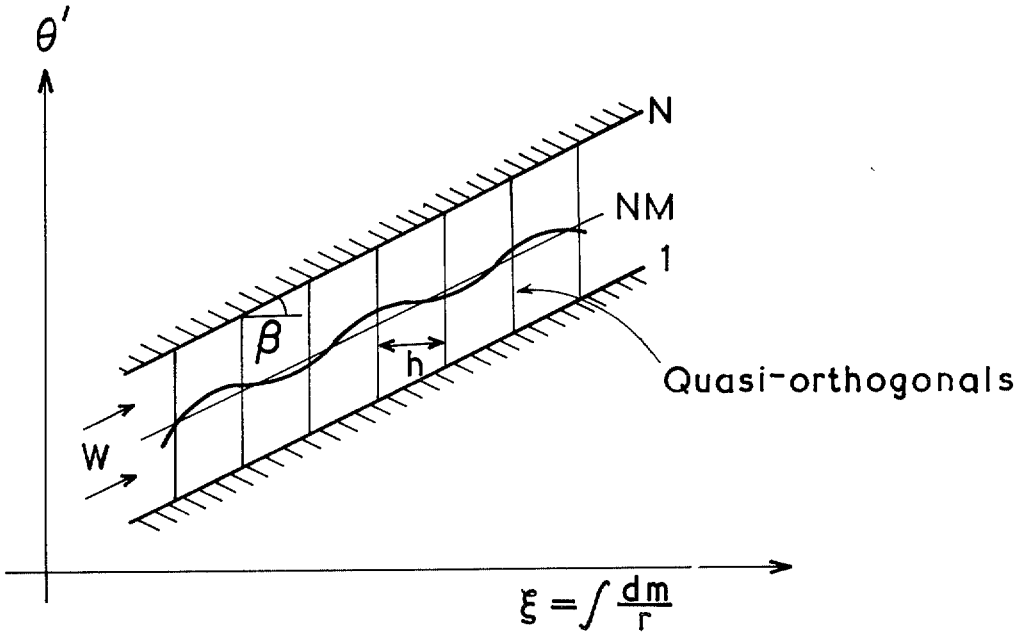

FIG. 2. Simple model of inclined flow on a cylindrical meridional stream surface.

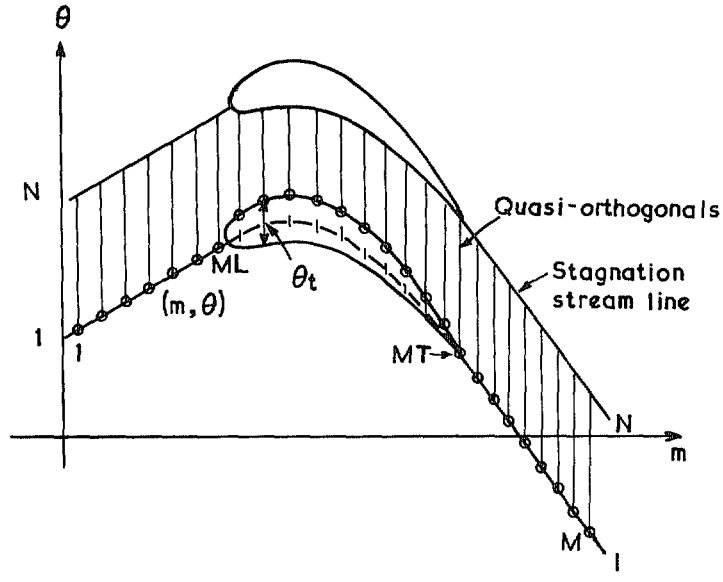

FIG. 3. Arrangement of quasi-orthogonals.

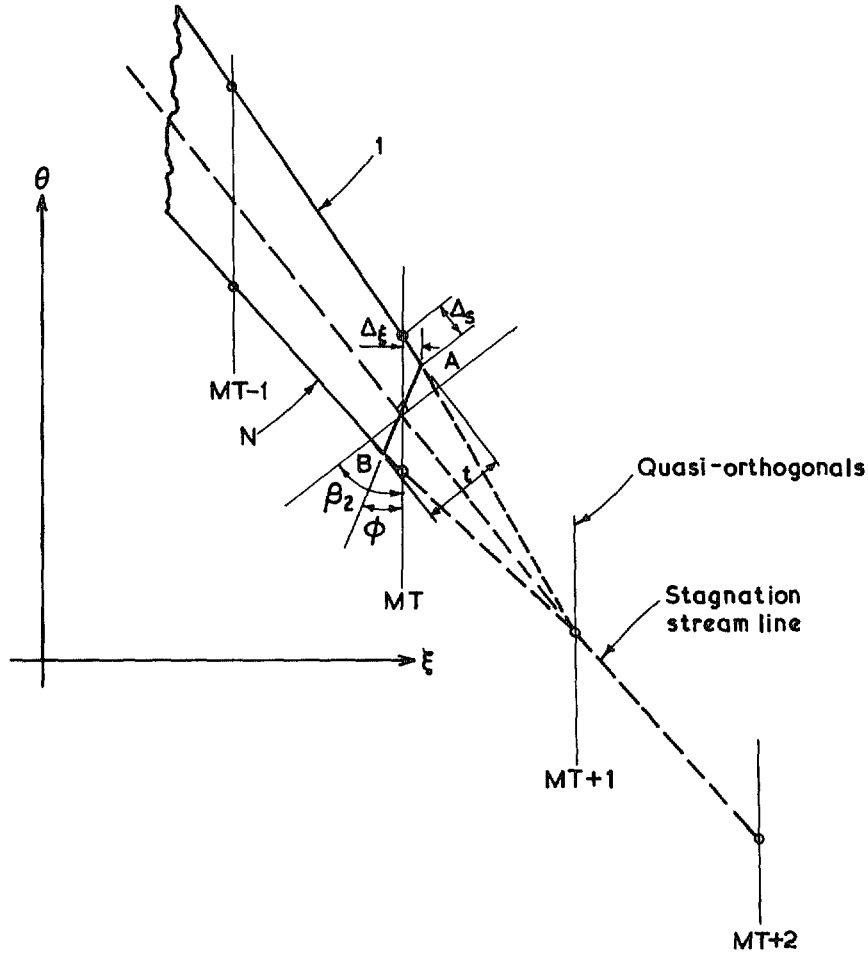

FIG. 4. The trailing edge region of a blade.

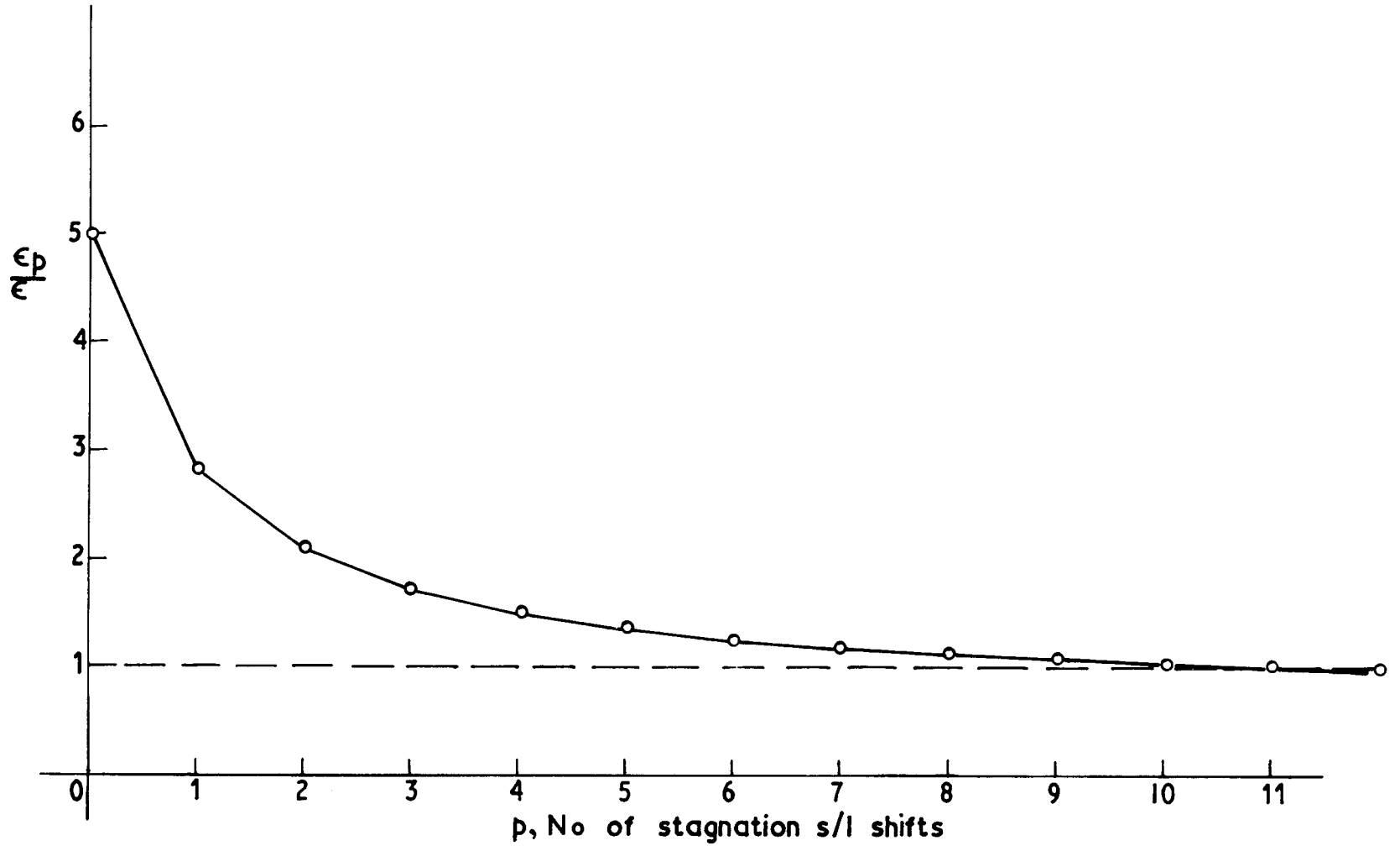

FIG. 5. Tolerance ~ streamline shifts.

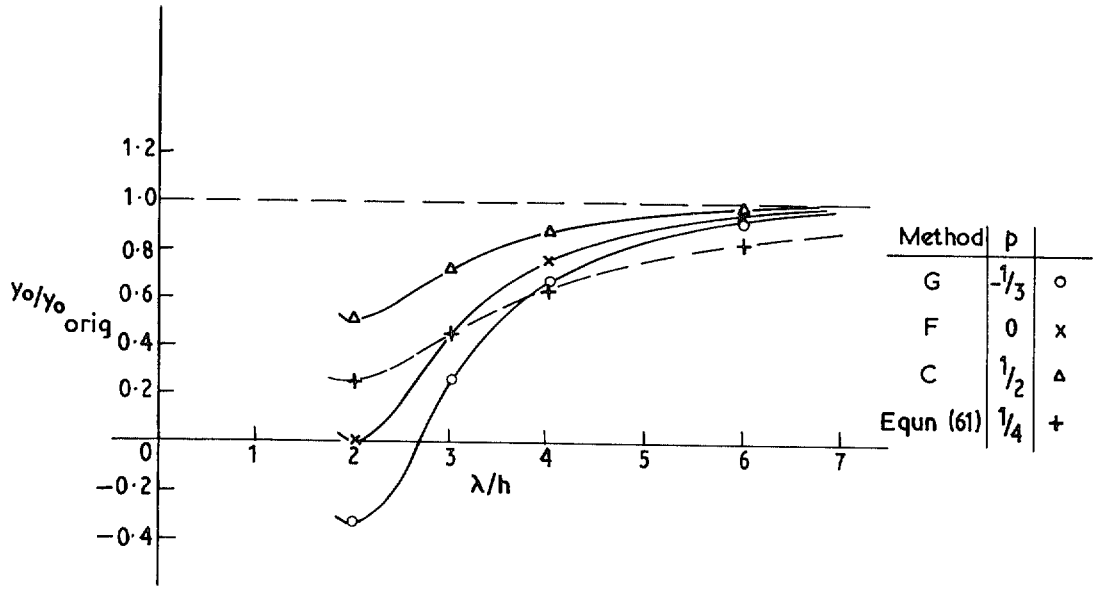

FIG. 6. Effect of smoothing processes.

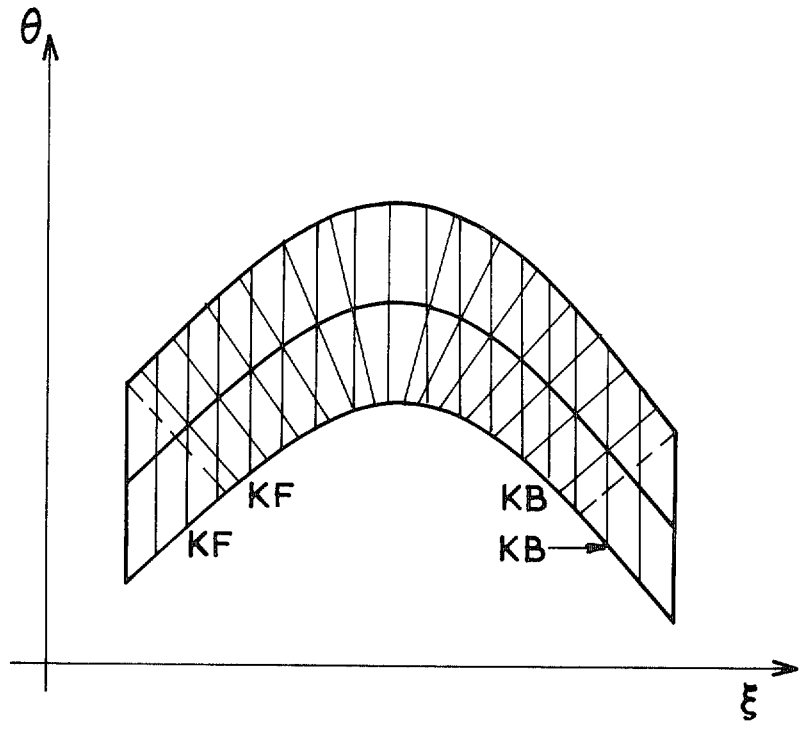

FIG. 7. Quasi-orthogonals and quasi-normals.

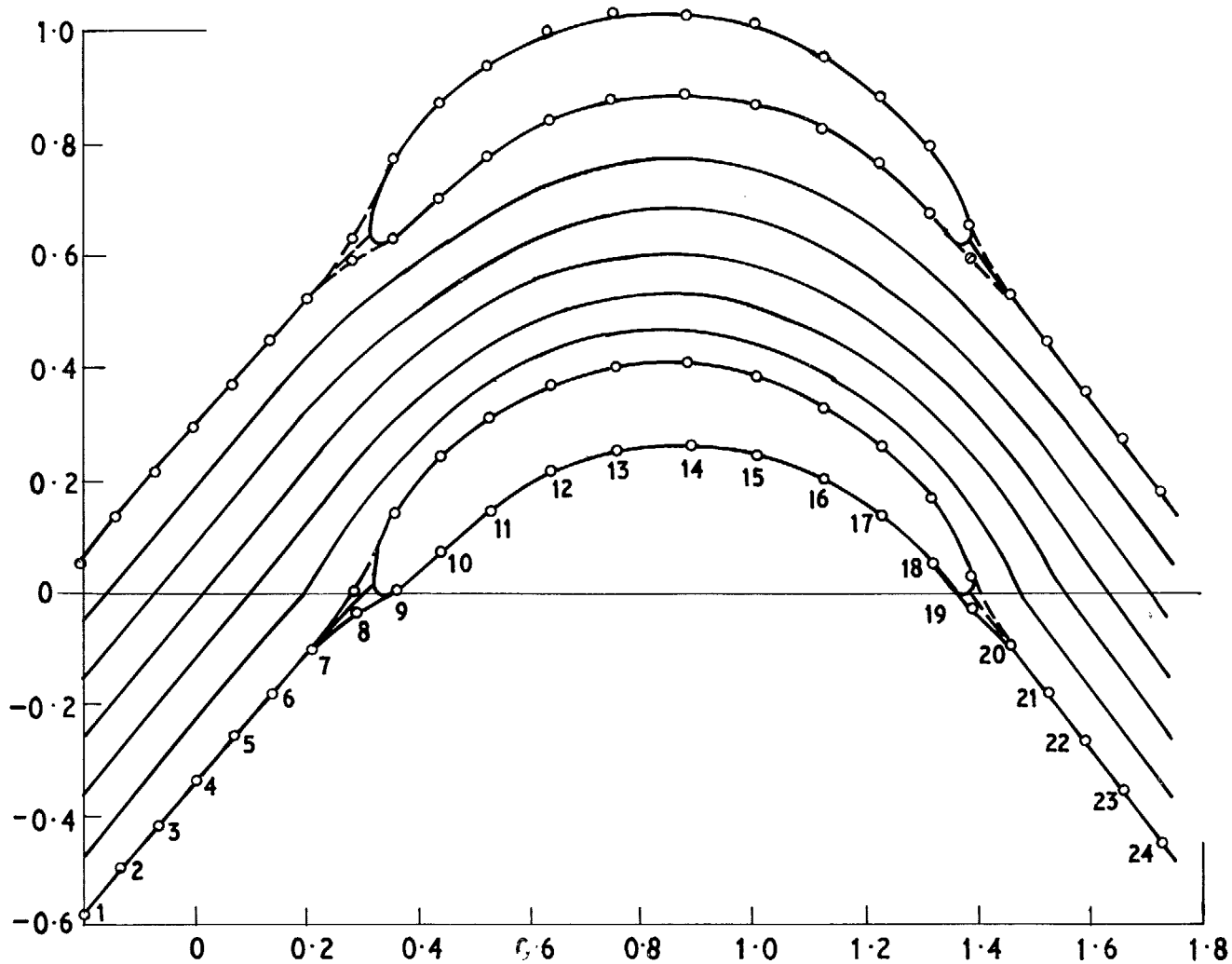

FIG. 8. 112° Camber section theoretical streamline.

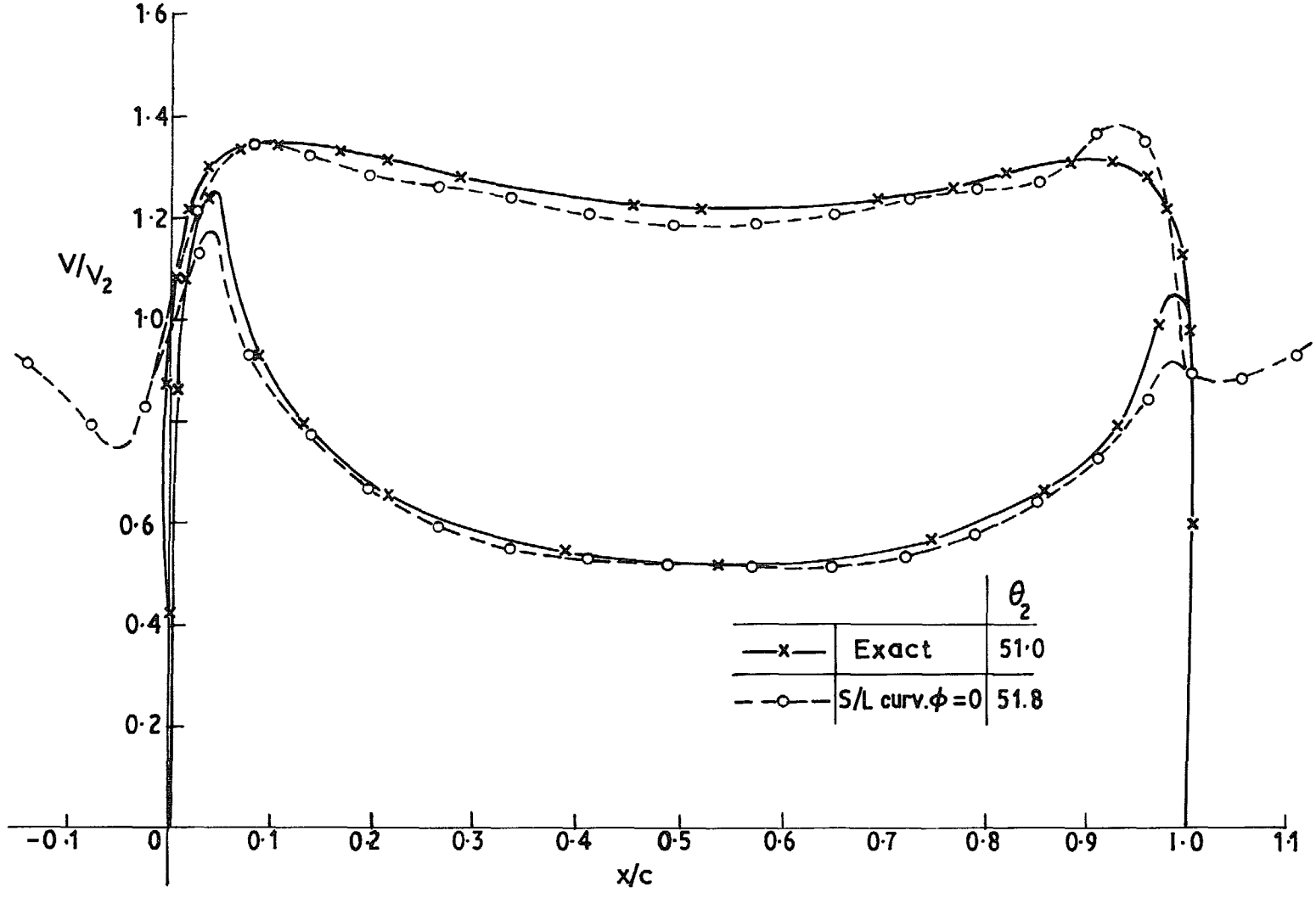

FIG. 9. 112° Camber section.

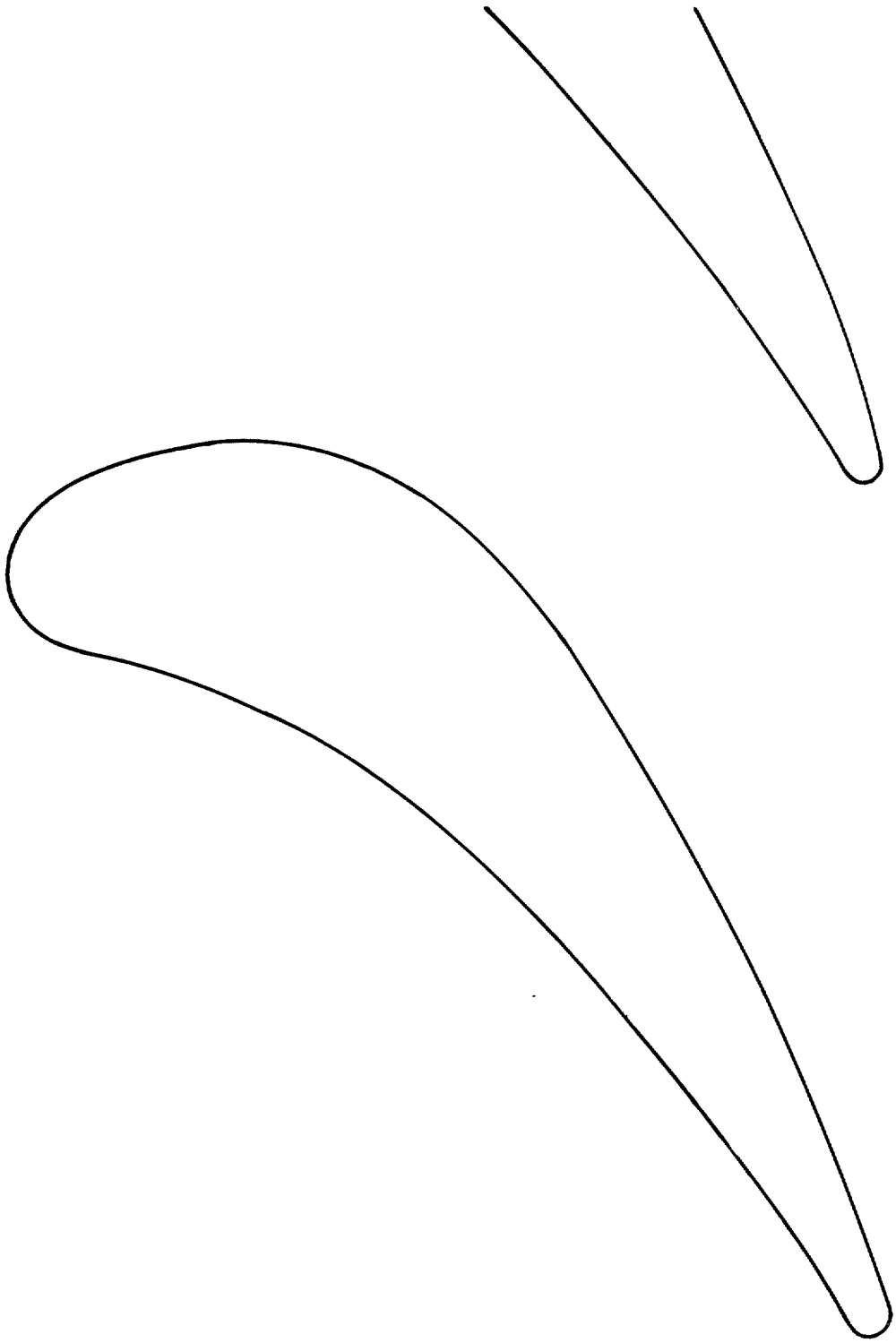

FIG. 10. Nasa TN D-3751 stator mean radius cascade.

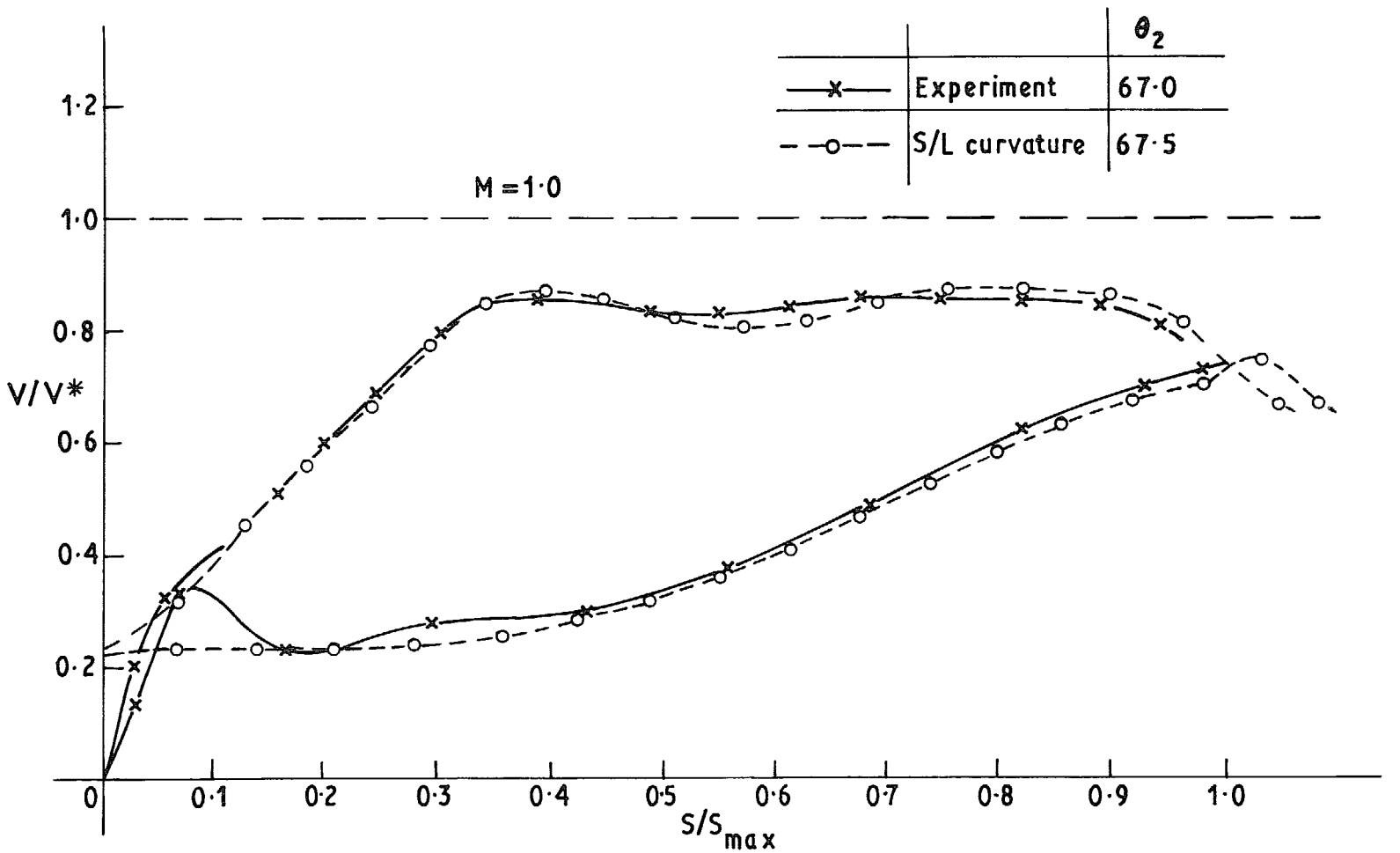

FIG. 11. Nasa TN D-3751 stator mean section design case $V/V^* = 0{\cdot}231$.

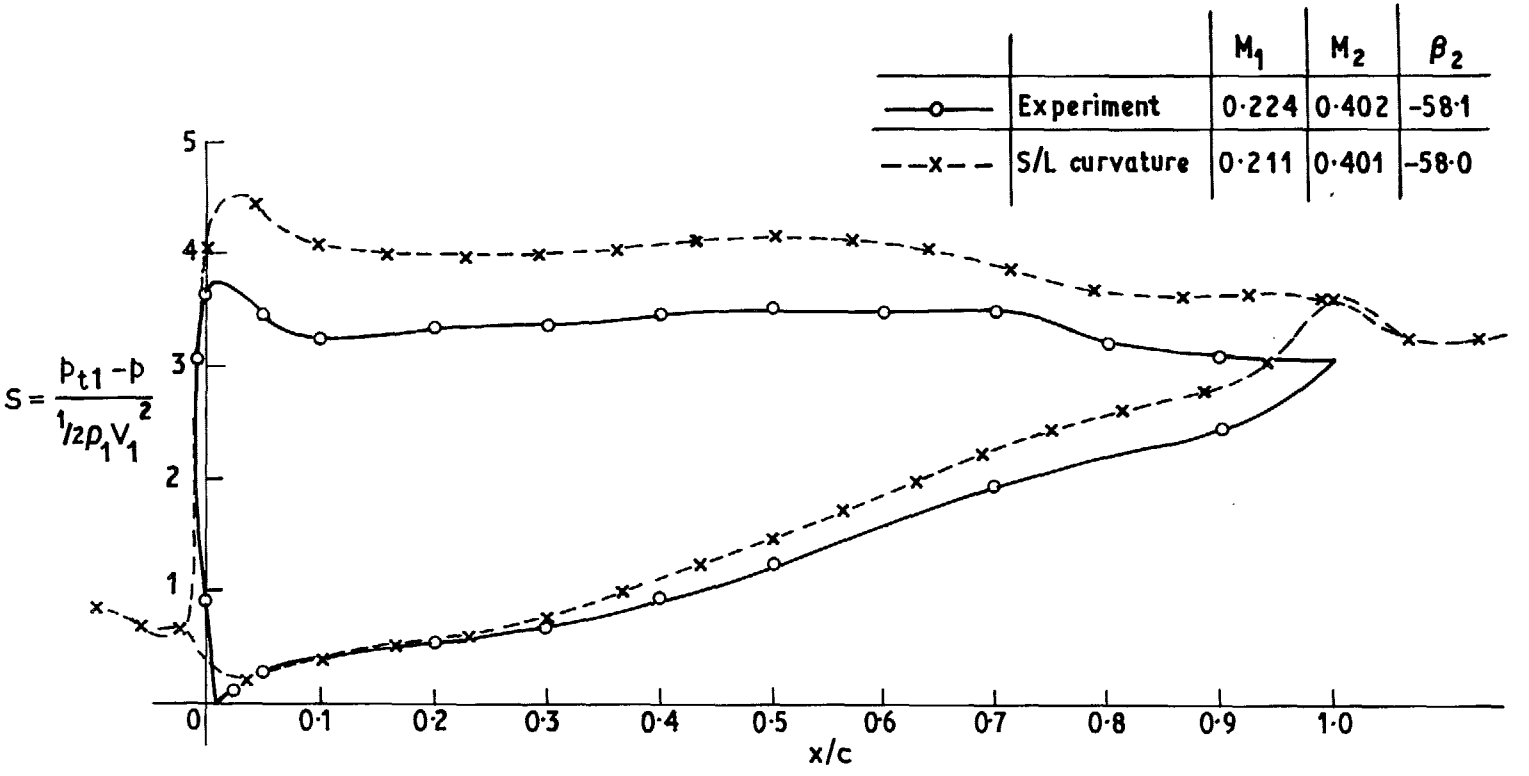

FIG. 12. Nasa primary series turbine blade, $\theta_c = 80°$, $\lambda = 38{\cdot}4°$, $\beta_1 = 20°$, pitch/chord = 0·556.

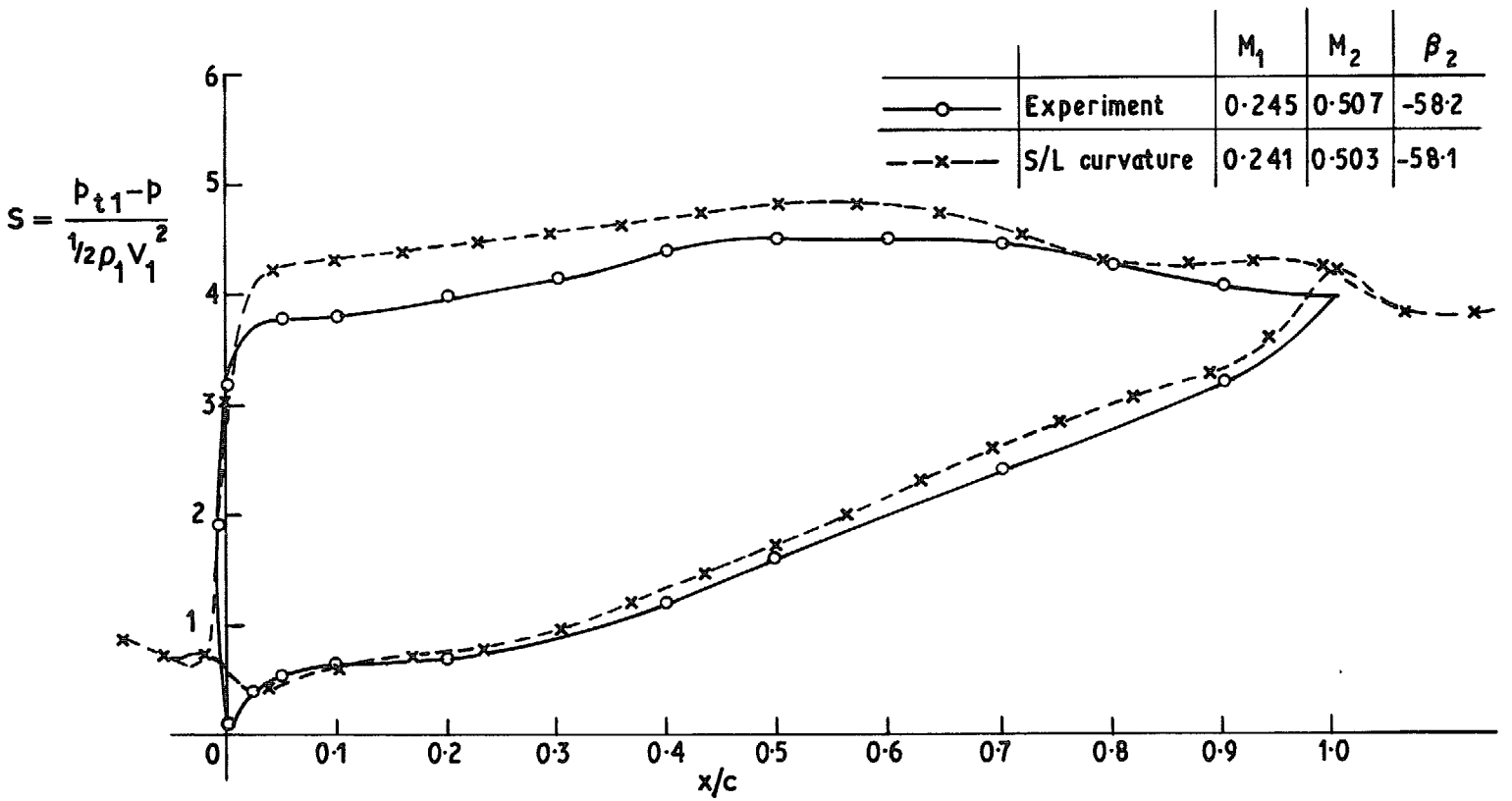

FIG. 13. Nasa primary series turbine blade, $\theta_c = 80°$, $\lambda = 38{\cdot}4°$, $\beta_1 = 10°$, pitch/chord = 0·556.

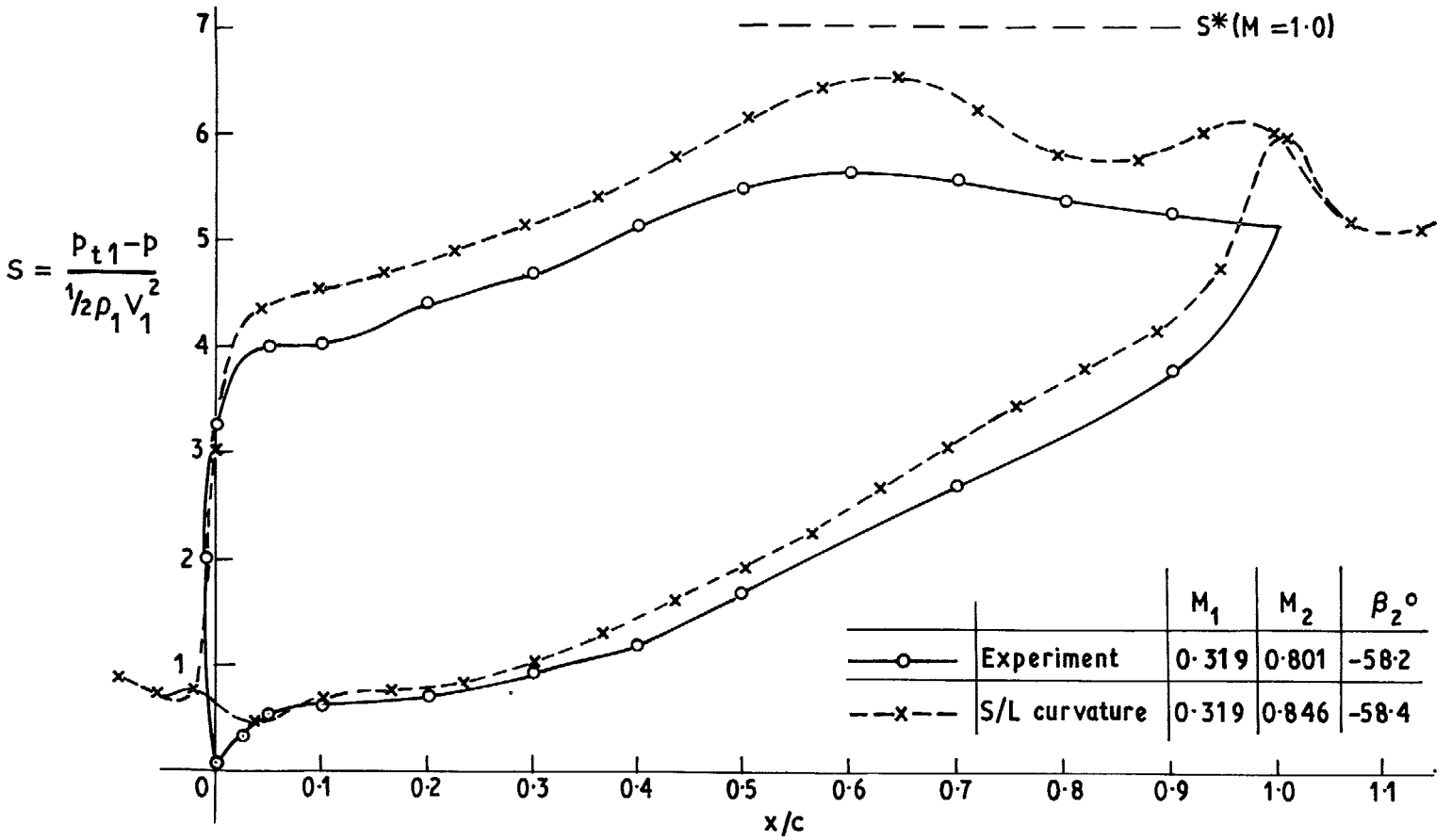

FIG. 14. Nasa primary series turbine blade, $\theta_c = 80°$, $\lambda = 38{\cdot}4°$, $\beta_1 = 10°$, pitch/chord = 0·556.

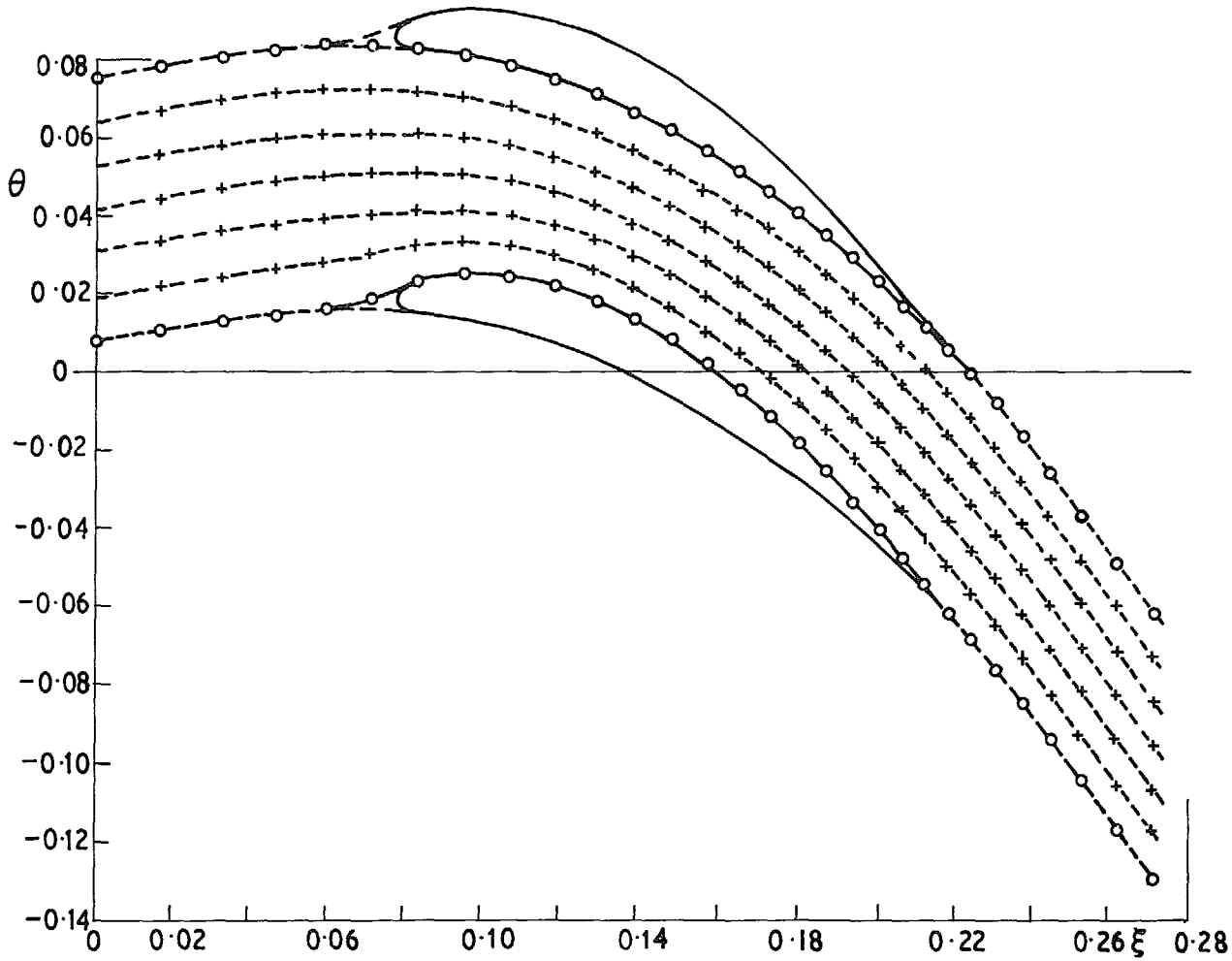

FIG. 15. 45° Flare case theoretical relative streamlines for rotating blade.

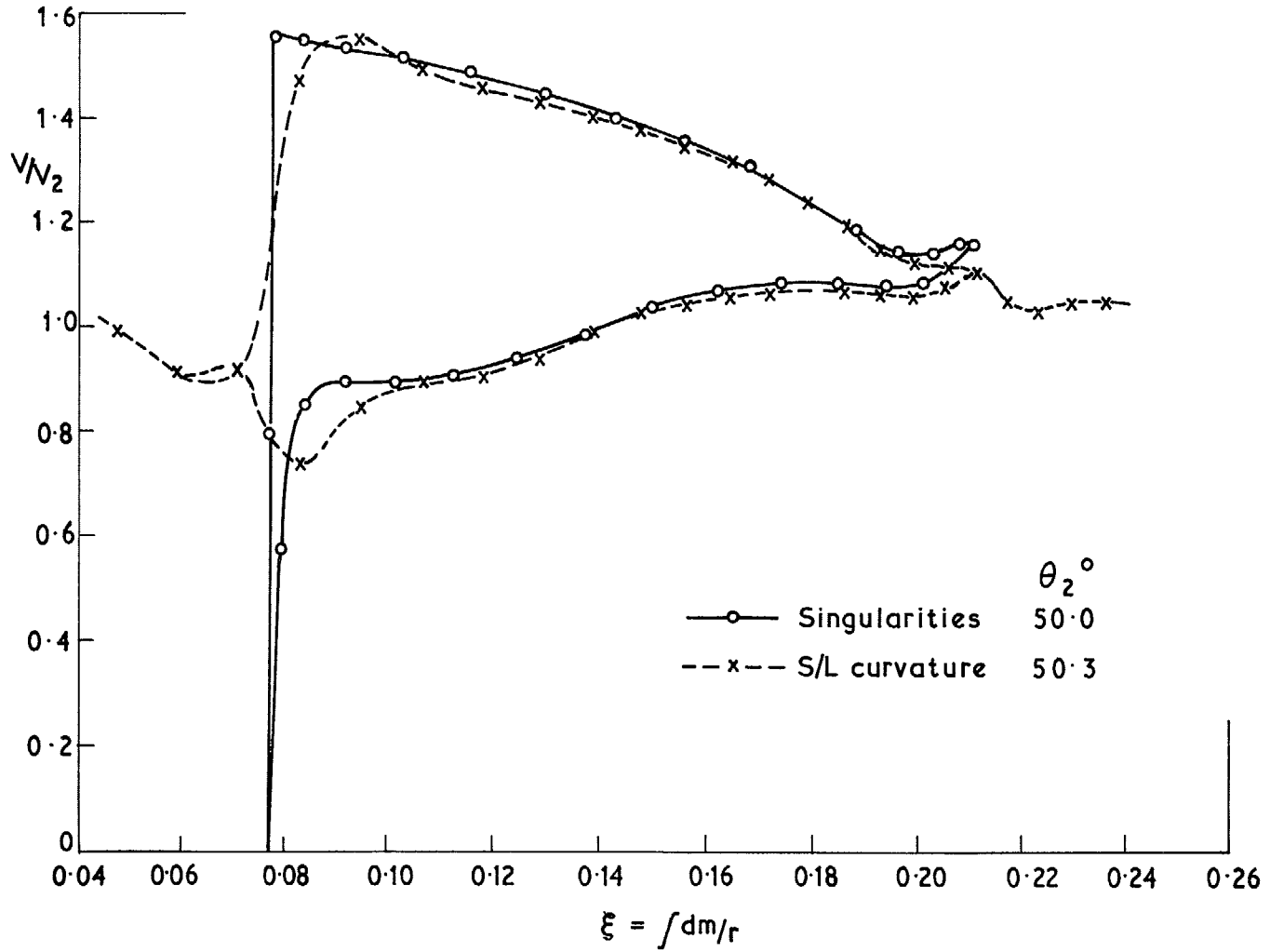

FIG. 16. 45° Flare case fixed blade $\theta_1 = 10°$ Low Mach No.

Printed in England for Her Majesty's Stationery Office by J. W. Arrowsmith Ltd., Bristol.
Dd. 503426 K.5 8/72

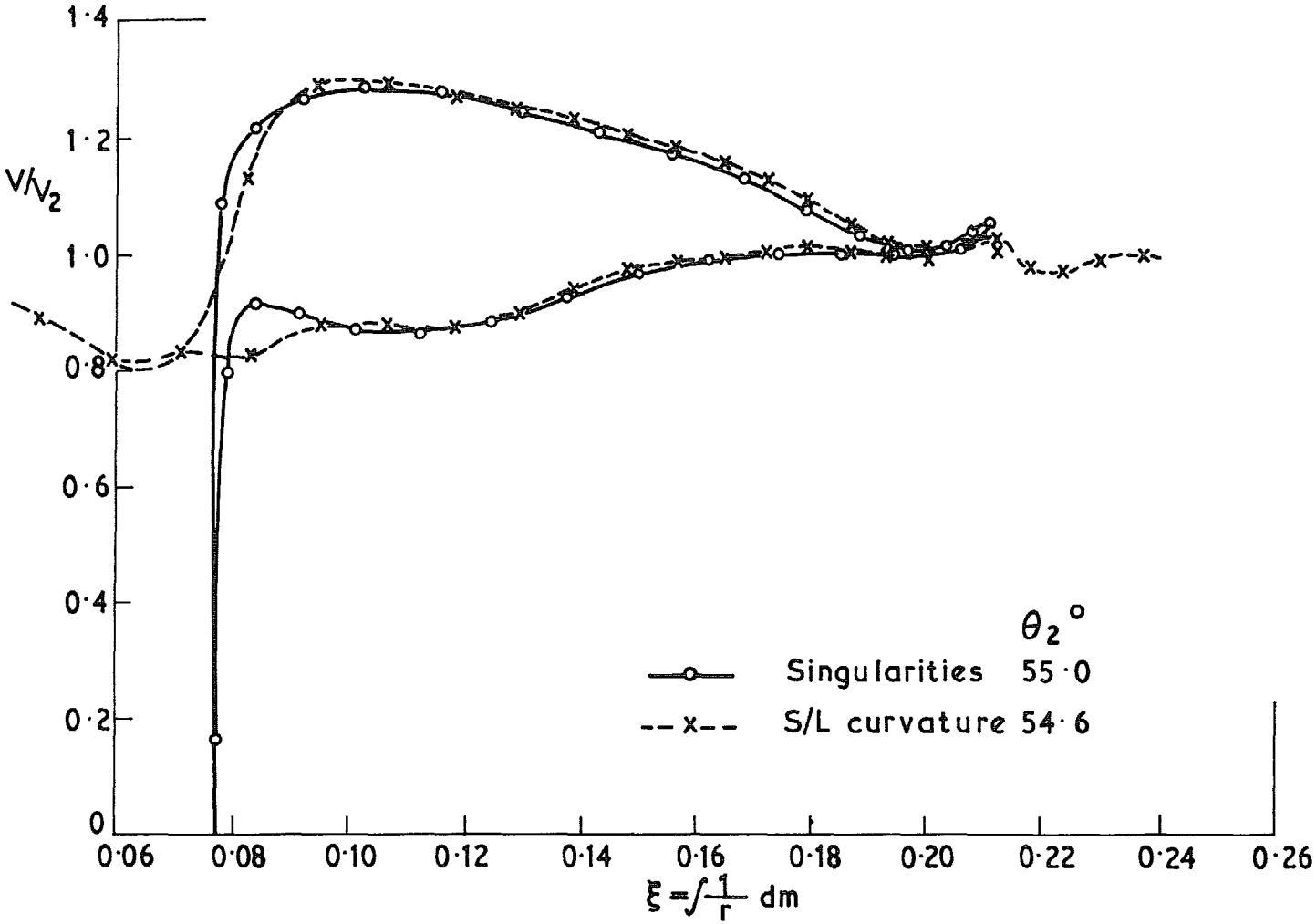

FIG. 17. 45° Flare case rotating blade $\theta_1 = 10°$ Low Mach No.

HER MAJESTY'S STATIONERY OFFICE

Government Bookshops

49 High Holborn, London WC1V 6HB
13a Castle Street, Edinburgh EH2 3AR
109 St Mary Street, Cardiff CF1 1JW
Brazennose Street, Manchester M60 8AS
50 Fairfax Street, Bristol BS1 3DE
258 Broad Street, Birmingham B1 2HE
80 Chichester Street, Belfast BT1 4JY

Government publications are also available through booksellers